Tectonic evolution of the active Hikurangi subduction margin, New Zealand, since the Oligocene.

A. Nicol, C. Mazengarb, Franck Chanier, G. Rait, C. Uruski, L. Wallace

Tectonic evolution of the active Hikurangi subduction margin, New Zealand, since the Oligocene

Andrew Nicol,[1] Colin Mazengarb,[2] Frank Chanier,[3] Geoff Rait,[4] Chris Uruski,[1] and Laura Wallace[1]

Received 30 November 2006; revised 21 February 2007; accepted 28 March 2007; published 6 July 2007.

[1] Deformation across the active Hikurangi subduction margin, New Zealand, including shortening, extension, vertical-axis rotations, and strike-slip faulting in the upper plate, has been estimated for the last ~24 Myr using margin-normal seismic reflection lines and cross sections, strike-slip fault displacements, paleomagnetic declinations, bending of Mesozoic terranes, and seafloor spreading information. Post-Oligocene shortening in the upper plate increased southward, reaching a maximum rate of 3–8 mm/year in the southern North Island. Upper plate shortening is a small proportion of the rate of plate convergence, most of which (>80%) accrued on the subduction thrust. The uniformity of these shortening rates is consistent with the near-constant rate of displacement transfer (averaged over ≥5 Myr) from the subduction thrust into the upper plate. In contrast, the rates of clockwise vertical-axis rotations of the eastern Hikurangi Margin were temporally variable, with ~3°/Myr since 10 Ma and ~0°–1°/Myr prior to 10 Ma. Post 10 Ma, the rates of rotation decreased westward from the subduction thrust, which resulted in the bending of the North Island about an axis at the southern termination of subduction. With rotation of the margin and southward migration of the Pacific Plate Euler poles, the component of the margin-parallel relative plate motion increased to the present. Plate convergence dominated the Hikurangi Margin before ca. 15 Ma, with the rate of margin-parallel motion increasing markedly since 10 Ma. Vertical-axis rotations could accommodate all margin-parallel motion before 1–2 Ma, eliminating the requirement for large strike-slip displacements (for example, >50 km) in the upper plate since the Oligocene. **Citation:** Nicol, A., C. Mazengarb, F. Chanier, G. Rait, C. Uruski, and L. Wallace (2007), Tectonic evolution of the active Hikurangi subduction margin, New Zealand, since the Oligocene, *Tectonics*, *26*, TC4002, doi:10.1029/2006TC002090.

1. Introduction

[2] Deformation in the Earth's crust is focused in plate boundary zones and directly reflects the relative motion of tectonic plates in juxtaposition. At many of the world's plate boundaries the first-order plate velocities and their temporal evolution are constrained by seafloor spreading data [e.g., *Stock and Molnar*, 1982; *DeMets et al.*, 1994; *Sutherland*, 1995; *Cande and Stock*, 2004] and, increasingly, by plate-wide geodetic measurements [e.g., *Beavan et al.*, 2002]. In cases where the geometry and kinematics of a boundary change abruptly, however, details of how strains accumulate across the boundary zone and evolve through time are often best determined by the analysis of the deformation in the zone. Resolving what controls these changes and the mechanisms by which they are achieved is important for improving our understanding of plate boundary processes. In this paper we consider these questions by charting the development of the active Hikurangi subduction margin, New Zealand, over the last 24 Myr.

[3] The Hikurangi Margin presently accommodates the oblique subduction of the Pacific Plate beneath the Australian Plate in the North Island of New Zealand (Figure 1). The margin occupies the transition from the subduction of the Pacific plate along the Tonga-Kermadec Trench (and associated back-arc extension in the Lau-Havre Trough) to the continental collision and strike-slip along the Alpine Fault (Figure 1). Subduction is inferred to have commenced about 24–30 Ma [*Ballance*, 1976; *Rait et al.*, 1991; *Kamp*, 1999; *Stern et al.*, 2006] and currently accommodates a relative plate-motion vector of 42–48 mm/year trending at ca. 50° to the trend of the margin (Figure 1). Plate convergence (i.e., margin-normal motion) is principally accommodated on the subduction thrust, while the remainder of the margin-normal motion and most of the margin-parallel motion (>50%) are accommodated in the upper plate through a combination of reverse faulting, strike-slip faulting, and vertical-axis clockwise rotations [*Wright and Walcott*, 1986; *Lamb*, 1988; *Walcott*, 1989; *Cashman et al.*, 1992; *Beanland*, 1995; *Kelsey et al.*, 1995, 1998; *Barnes and Mercier de Lépinay*, 1997; *Barnes et al.*, 1998; *Beanland and Haines*, 1998; *Beanland et al.*, 1998; *Little et al.*, 1998; *Nicol et al.*, 2002; *Nicol and Beavan*,

[1]GNS Science, Lower Hutt, New Zealand.
[2]Mineral Resources Tasmania, Rosny Park, Australia.
[3]UMR CNRS - 8110, Processus et Bilans des Domaines Sédimentaires, Université des Sciences et Technologies de Lille 1, Villeneuve d'Ascq Cedex, France.
[4]Talisman Energy, Calgary, Alberta, Canada.

0278-7407/07/2006TC002090

2003; *Wallace et al.*, 2004; *Rowan et al.*, 2005; *Nicol and Wallace*, 2007; R. I. Walcott and T. C. Mumme, Paleomagnetic study of the tertiary sedimentary rocks from the East Coast of the North Island, New Zealand, unpublished report, 1982, hereinafter referred to as Walcott and Mumme, 1982] (Figure 1). Therefore upper plate deformation provides important constraints on the timing and kinematics of Hikurangi Margin subduction.

[4] Previous studies have focused only on part of the Hikurangi Margin or on one component of the deformation field, while tectonic reconstructions of the plate boundary zone are typically constrained by the spatial distribution of

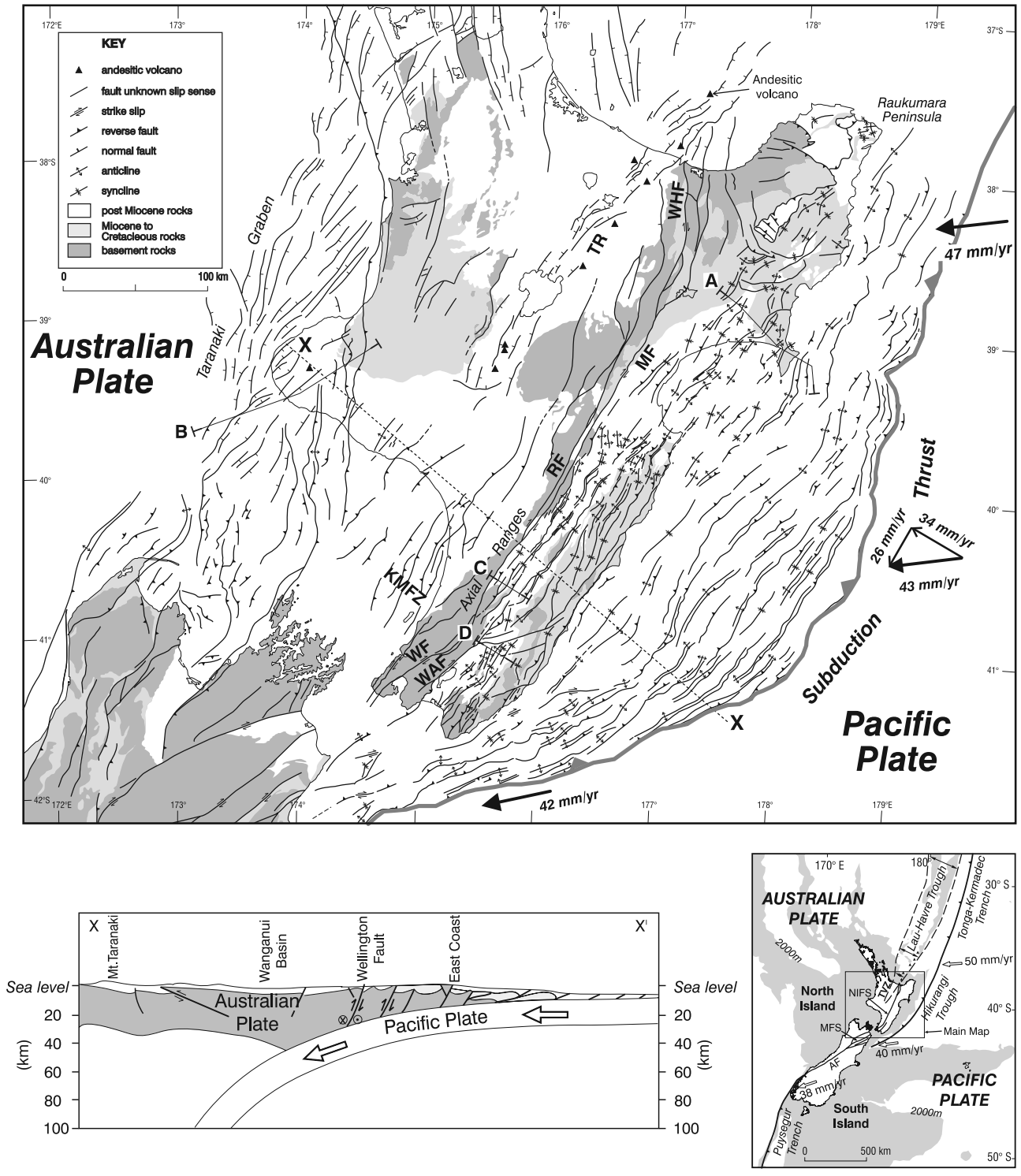

Figure 1

Mesozoic basement terranes and Cenozoic sedimentary facies, paleomagnetic rotations, and/or seafloor spreading data [e.g., *Ballance*, 1976; *Walcott*, 1978, 1984a, 1987; *Cole*, 1986; *Kamp*, 1987, 1999; *Lamb*, 1988; *Lewis and Pettinga*, 1993; *Beanland*, 1995; *Field et al.*, 1997; *King*, 2000]. The resulting tectonic reconstructions of the Hikurangi Margin can vary significantly and incorporate a wide range of fault strike-slip, margin-normal shortening/extension, and rotations about vertical axes. In this paper we attempt to reduce some of the uncertainty inherent in our understanding of margin deformation by collating and analyzing mainly Miocene and younger strain data. To place first-order constraints on the evolution of the margin since its inferred inception, we use strain profiles normal to the margin, together with strike-slip on individual faults and rotations about vertical axes measured using paleomagnetic declinations. Our estimates of the magnitudes, styles, and spatial distribution of deformation are reconciled with GPS and seafloor spreading estimates of the relative plate motion vector.

[5] Determining the spatial and temporal accumulation of strain in the overriding Australian Plate at the Hikurangi Margin is possible because Miocene and younger horizons (i.e., strain markers) can be mapped across most of the width of the plate boundary zone using outcrop, seismic reflection lines, and gravity profiles. These horizons are mainly part of a late Cretaceous-Quaternary marine sequence that reaches thicknesses of up to 8 km and rests with angular unconformity on Mesozoic basement rocks [see *King and Thrasher*, 1996; *Field et al.*, 1997, and references therein] (Figure 2). Late Cretaceous and younger strata are commonly laterally discontinuous on a scale of tens of kilometers due to differential uplift and subsidence, fluctuations in sea level, and lateral changes in the environment of deposition. Biostratigraphy of the Cenozoic sequence is, however, well established and allows temporal marker horizons to be traced over distances of hundreds of kilometers [e.g., see *King and Thrasher*, 1996; *Field et al.*, 1997].

[6] Our analysis suggests that vertical-axis rotations, strike-slip faulting, and shortening in the overriding Australian Plate since the Oligocene may have been lower than previously thought. The principal reasons for this are that (1) new data and analysis indicate that rotations of the margin are low (45°–50° as opposed to 60°–90°), (2) a significant component (>50%) of the margin-parallel plate motion was accommodated by rotations (decreasing the strike-slip faulting required) and, (3) most (>80%) of the plate convergence across the plate boundary accrued on the subduction thrust, and therefore is not manifested as a deformation in the upper plate [*Nicol and Beavan*, 2003; *Wallace et al.*, 2004; *Nicol and Wallace*, 2007; this study].

2. Shortening and Extension

[7] Geological cross sections (Figure 2), seismic reflection lines, gravity profiles, and fault-displacement rates have been used to measure margin-normal extension and shortening for the top 2–6 km of the crust in the overriding Australian Plate. The data used to construct the 54 cross sections used in this paper are presented on a GNS website (http://www.gns.cri.nz/research/basindynamics/strainprofiledata.html). These cross sections are typically oriented approximately normal to the trend of, and distributed across, the margin (Figures 3 and 4). Each profile contains one or more horizons of Miocene or younger age ($\leq$24 Ma) from which components of dip-slip normal or reverse fault displacements and folding were estimated (for example, Figure 2). In order to measure the extension and shortening from profiles we have assumed that predeformation bed dips were horizontal, that the measured fault dips can be projected below the available data, and that unresolved small faults do not account for a significant component of the total strain budget (i.e., $\leq$10%). Because much of the strike-slip faulting within the Hikurangi Margin is confined to the North Island Fault System (as defined by *Mouslopoulou et al.*, 2007; this fault system is also referred to as the North Island Dextral Fault Belt or the North Island Shear Belt, see *Beanland*, 1995), we infer that folding resulting from distributed strike-slip (rather than contraction) was not significant [cf. *Tikoff and Peterson*, 1998]. We can neither, however, discount the possibility that some folding formed due to the strike-slip in the North Island Fault System nor that local strike-slip has resulted in errors in horizon correlation across this system. Uncertainties in the strain estimates, which typically range from 20–50%, arise mainly because of measurement errors

Figure 1. Present tectonics of the New Zealand Plate boundary. The Hikurangi Margin (enclosed by the box) forms the transition from continental collision along the Alpine Fault to subduction with back-arc extension along the Tonga-Kermadec Margin. Location of the main map is shown in inset map. Regional geological map shows the locations and types of structures that deform Miocene and younger rocks across the Hikurangi Margin. Data from *New Zealand Geological Survey* [1972], *Anderton* [1981], *Melhuish* [1990], *Cashman et al.* [1992], *Kelsey et al.* [1993, 1995], *Lewis and Pettinga* [1993], *Davey et al.* [1995], *Thrasher et al.* [1995], *Begg and Mazengarb* [1996], *King and Thrasher* [1996], *Barnes and Mercier de Lépinay* [1997], *Field et al.* [1997], *Uruski* [1998], *Begg and Johnston* [2002], *Lamarche et al.* [2000], *Mazengarb and Speden* [2000], *Edbrooke* [2001], *Barnes et al.* [2002], *Lee and Begg* [2002], and Edbrooke (2003, personal communication, QMAP Waikato unpublished data). Shading in the North Island shows the extent of Mesozoic basement (dark grey), post-Cretaceous to Miocene (light grey) and post-Miocene (white) rocks. Locations of the cross sections in Figure 3 are shown. Regional cross section X-X′ modified from the work of *Nicol and Beavan* [2003]. Relative plate motion vectors from *Beavan et al.* [2002], with margin-normal (34 mm/year) and margin-parallel (26 mm/year) components shown for central margin. Abbreviations main map: KMFZ, Kapiti-Manawatu Fault Zone; MF, Mohaka Fault; RF, Ruahine Fault; TR, Taupo Rift; WAF, Wairarapa Fault; WF, Wellington Fault; WHF, Whakatane Fault. Abbreviations inset map: AF, Alpine Fault; MFS, Marlborough Fault System; NIFS, North Island Fault System; TVZ, Taupo Volcanic Zone.

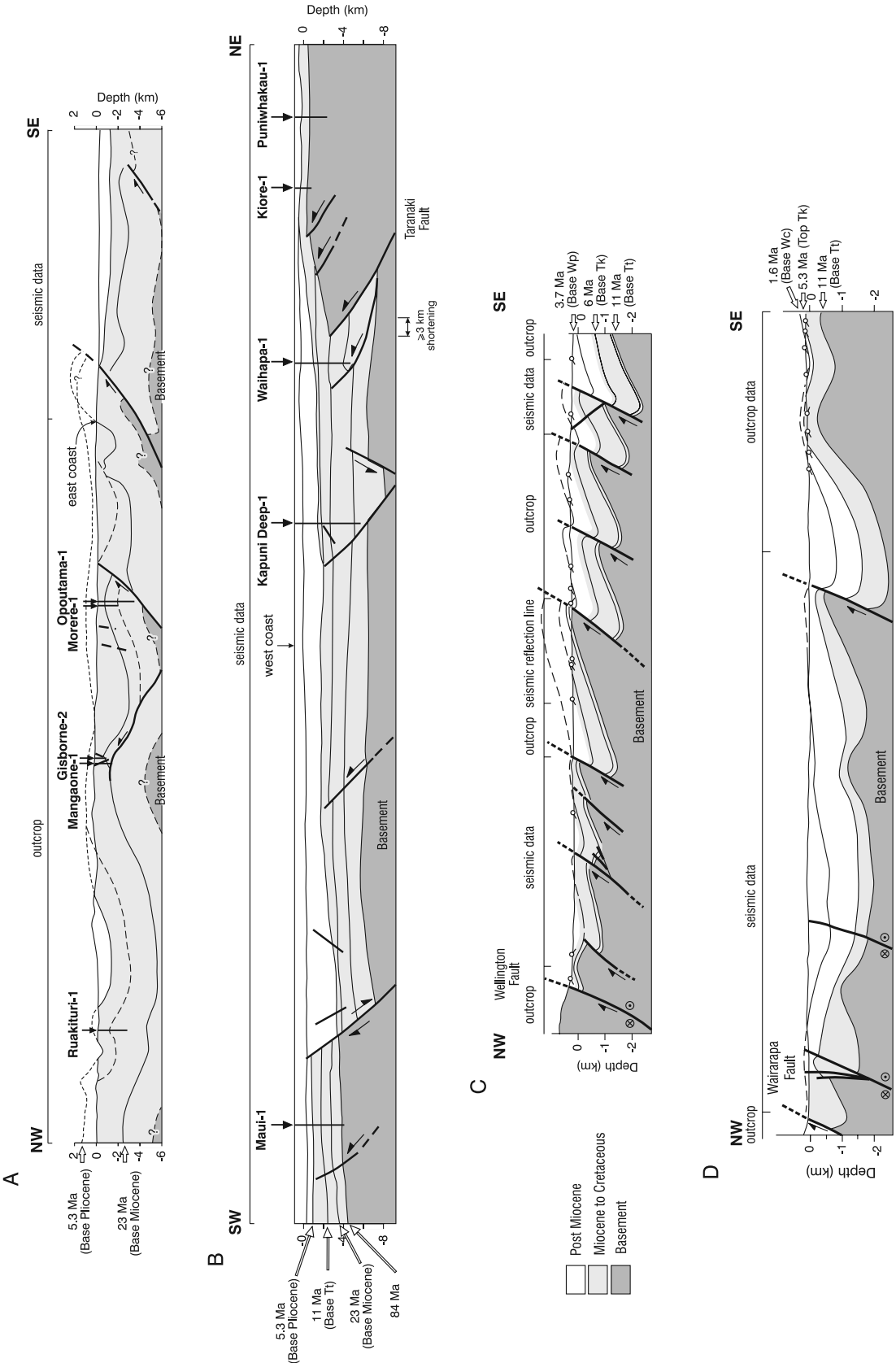

Figure 2. Examples of cross sections constructed from seismic reflection, drill hole, and outcrop data. (a) northern Hawkes Bay (modified from *Mazengarb and Speden* [2000]), (b) Taranaki Basin (modified from cross section D-D′ of *Thrasher et al.* [1995]), (c) Eketahuna (modified from *Lamarche et al.* [1995], with additional data from *Kelsey et al.*, 1995 and this study), (d) Wairarapa (modified from *Cape et al.* [1990]), with additional mapping from Nicol (unpublished data, 1996–1999). Tadpoles on cross sections C-C′ and D-D′ indicate bed dips in the plane of the section. Cross-section locations indicated on Figure 1. Cross-section A, B, C, and D used for strain estimates in profiles 21 and 51, 57–59, 9 and 41, and 8 and 40, respectively.

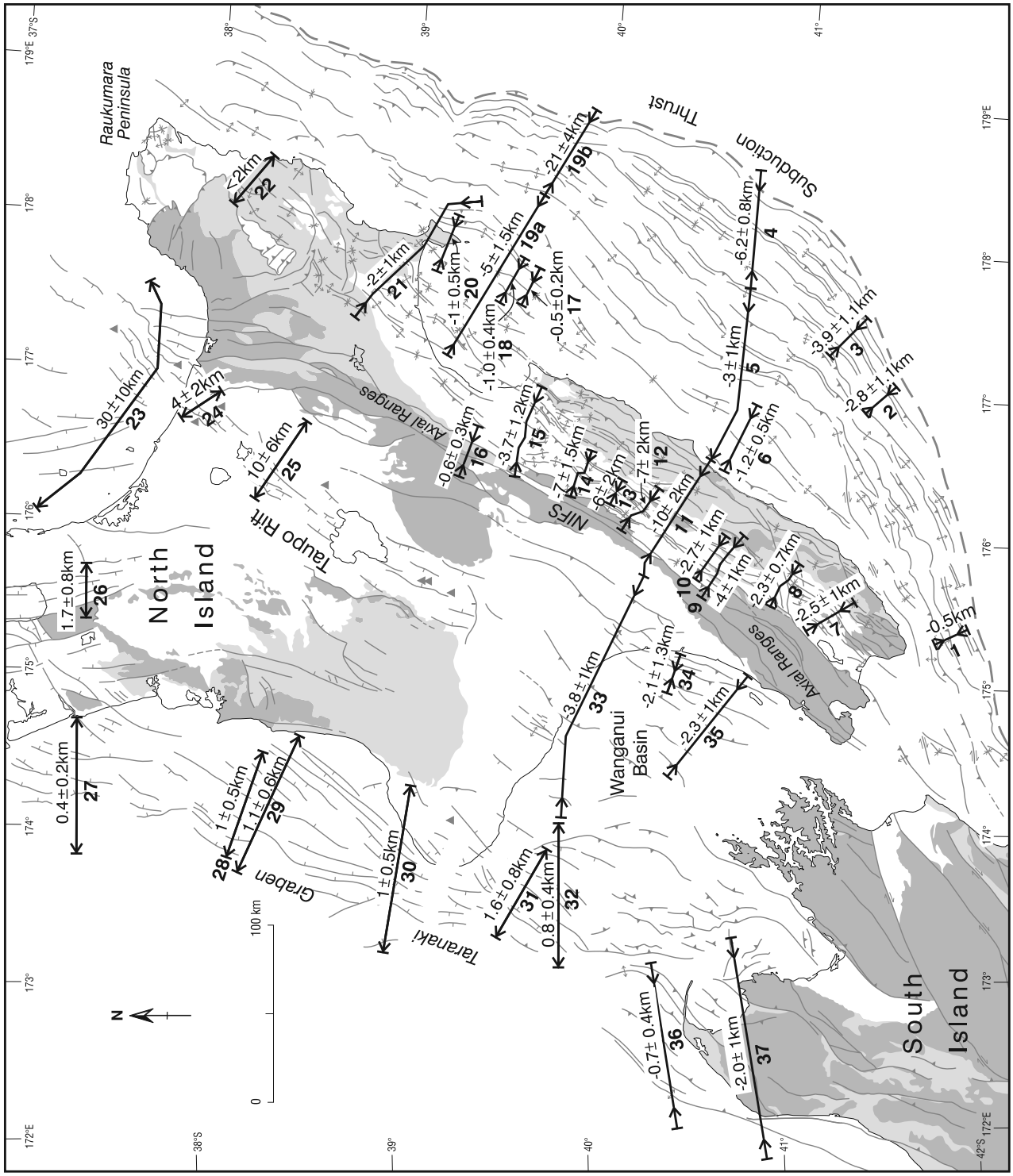
Raukumara Peninsula
North Island
South Island
Taupo Rift
Axial Ranges
NIFS
Wanganui Basin
Graben
Taranaki
Thrust
Subduction
N
0
100 km
<2km
22
-2±1km
21
-1±0.5km
20
-1±0.4km
18
-.5±1.5km
19a
-21±4km
19b
-0.5±0.2km
17
30±10km
23
4±2km
24
10±6km
25
-0.6±0.3km
16
-3.7±1.2km
15
-7±1.5km
14
-6±2km
13
-7±2km
12
-10±2km
11
-6.2±0.8km
4
-3±1km
5
-1.2±0.5km
6
-3.9±1.1km
3
-2.8±1.1km
2
-0.5km
1
-2.7±1km
9
-4±1km
10
-2.3±0.7km
8
-2.5±1km
7
1.7±0.8km
26
0.4±0.2km
27
1±0.5km
28
1.1±0.6km
29
1±0.5km
30
1.6±0.8km
31
0.8±0.4km
32
-3.8±1km
33
-2.1±1.3km
34
-2.3±1km
35
-0.7±0.4km
36
-2.0±1km
37

Figure 3

introduced by uncertainties in fault dips (for example, ±10°–20°) and bed dips beneath reverse faults. We have principally used line-length measurements to estimate extension and contraction in each section. Given the limited number of well-constrained horizons in some sections and the prospect of a component of strike-slip on some faults, in most cases, more sophisticated area-balancing techniques were unwarranted. Horizon ages are mainly from the micropaleontological definition of New Zealand stages where strata crop out or are intersected in wells. Ages for New Zealand stage boundaries are given by *Cooper* [2004]. Further information on the sources of the profile data (for example, Figure 2), horizon dating, and details of the methodology are given in the supplementary electronic data set lodged on the GNS Science Web site http://www.gns.cri.nz/research/basindynamics/strainprofiledata.html.

[8] Extension and shortening that accumulated during the time intervals ~0–5 and ~5–24 Ma are presented on Figures 3 and 4, respectively. The spatial distribution and quantity of data is greatest for the last ca. 5 Myr (Figure 3). Due principally to erosion and intense deformation, Miocene marker horizons are mainly limited to the regions east of the Axial Ranges and west of the Taranaki Fault or Taupo Rift (Figures 1 and 4).

2.1. Pliocene-Pleistocene Deformation

[9] Within the plate boundary zone, both margin-normal extension and contraction have occurred since the Miocene (Figures 1, 2, 3, and 5). A northeast-southwest trending boundary divides the North Island in two and separates areas dominated by extension (northwest) and shortening (southeast) (Figure 5). The rates of extension and shortening increase with increasing distance from this boundary [*Beanland and Haines*, 1998; *Nicol and Wallace*, 2007; this study].

[10] Extensional faulting dominates in the Taupo Volcanic Zone, which continues north of New Zealand as the back-arc Lau-Havre Trough (Figure 1), and in the Taranaki Graben. Rifting in these areas is accompanied by andesitic and/or rhyolitic volcanism [*Cole et al.*, 1995; *King and Thrasher*, 1996] (Figure 3). The locus of volcanism and extension has migrated eastward since the middle Miocene, which could be due to the eastward rollback of the Pacific Plate [*Ballance*, 1976; *Walcott*, 1987]. The active Taupo Rift, which is within the Taupo Volcanic Zone, accommodates a maximum of 5–15 mm/year extension [*Villamor and Berryman*, 2001; *Wallace et al.*, 2004].

[11] South of the southern termination of the Taupo Rift, contraction mainly occurs within the axial ranges, in a zone ~20–50 km wide and immediately east of these ranges, and within 50 km of the subduction thrust at the seabed (Figures 1, 2, 3, 4, 5, and 6) [see also *Barnes and Mercier de Lépinay*, 1997; *Nicol and Beavan*, 2003]. High shortening within, and immediately east of, the axial ranges is supported by the strike-parallel horizon separation diagram in Figure 6 (see caption for description of the derivation of diagram). On the range crest, basement rocks are locally overlain by 2.4-Ma strata (Figure 6) from which we infer that the range crest is about 2.4 Ma in age. The 2.4-Ma horizon is downthrown to the east with up to 3 km of vertical separation on a reverse fault(s) and fold(s), while the vertical separation between range crest and the 3.7-Ma horizon is ≥4.7 km. Figure 6 indicates that the uplift of the axial ranges both predate and postdate 2.4 Ma and is consistent with the notion that uplift since 5 Ma accrued in two main time intervals, after ca. 1.5 and 2.5–3.7 Ma [*Melhuish*, 1990; *Beanland et al.*, 1998; *Nicol et al.*, 2002]. At approximately the southern end of the Taupo Volcanic Zone, high vertical separations step 100 km east of the axial ranges onto the Lachlan Fault (Figure 7), which accommodated ca. 3 km of vertical separation after 5 Ma (see cross section b-b′, *Barnes et al.*, 2002, Figure 16). This eastward shift in the loci of high shortening strains could be due in part to a change in the geometry of the downgoing plate (for example, an eastward shift in a kink in the plate which focuses upper plate deformation; cf. *Henrys et al.* [2006]), a change in the dimensions of the plate interface that has experienced stable sliding in the last 5 Myr and/or the presence of preexisting zones of weakness in the upper plate.

[12] High contractional strain occurs up to 50 km west of the subduction thrust at the seabed [*Davey et al.*, 1986a, 1986b; *Lewis and Pettinga*, 1993; *Barnes and Mercier de Lépinay*, 1997]. This zone of intense deformation is up to 4 km above the subduction thrust and contains a series of imbricate thrusts which locally splay from the plate interface (Figure 8). These thrusts can be regarded as being part of a subduction thrust zone, which may widen in relatively unconsolidated sedimentary rocks close to the seabed [*Nicol and Beavan*, 2003]. This interpretation is consistent with the high cumulative shortening (for example, 5–15 mm/year) across the zone [*Barnes and Mercier de Lépinay*, 1997, Figure 8], which is viewed here as being interplate and has not been included in the estimates of cumulative strain on profiles A–E (Figure 5, excluded subduction thrust zone marked). The downdip extension of this interplate deforming zone may be indicated by a weak low velocity layer of 3–4 km thickness [*Bannister*, 1988].

[13] Cumulative margin-normal strains in the upper plate and across the entire Hikurangi Margin after 5 Ma become increasingly extensional with distance northward from the southern termination of subduction (Figure 5). As much as 20-km shortening occurs in the south along profile D (Figure 5), while up to 42-km extension is interpreted on profile A across Raukumara Peninsula (Figure 5). These changes in the type and magnitude of deformation are consis-

Figure 3. Map showing the distribution of Pliocene and younger margin-normal shortening and extension. Strain profiles indicate margin-normal shortening (inward directed arrows and negative values) and extension (outward directed arrows and positive values). Shading in the North Island shows the extent of Mesozoic basement (dark grey), post-Cretaceous to Miocene (light grey) and post-Miocene (white) rocks. For description of data used to estimate strains in profiles, refer to website http://www.gns.cri.nz/research/basindynamics/strainprofiledata.html.

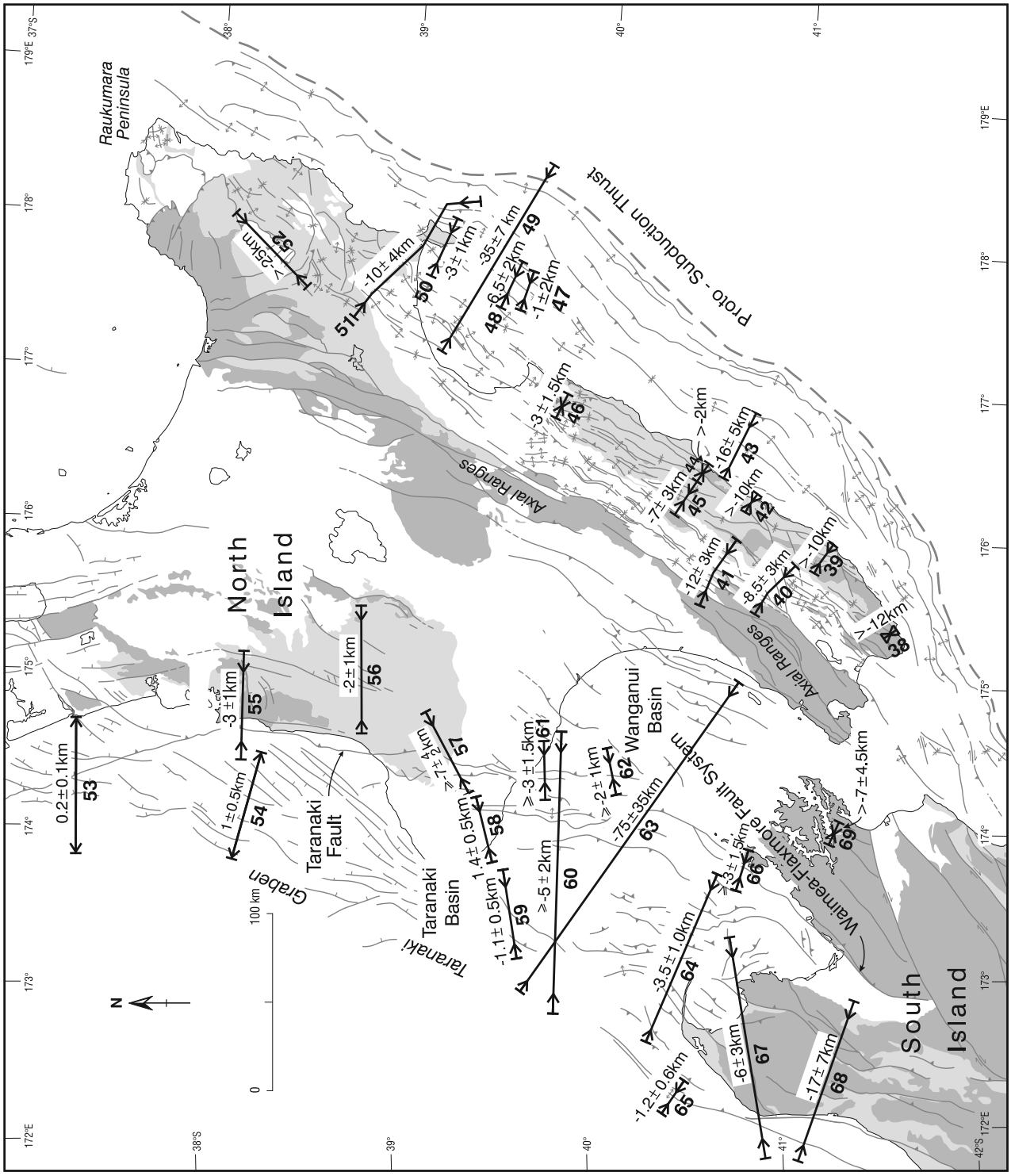
Raukumara Peninsula
Proto - Subduction Thrust
Axial Ranges
North Island
Taranaki Fault
Taranaki Basin
Taranaki
Wanganui Basin
Wairnea-Flaxmore Fault System
South Island
Axial Ranges
Axial Ranges
Graben
N
0
100 km
179°E 37°S
178°
177°
176°
175°
174°
173°
172°E
38°S
39°
40°
41°
42°S
172°E
179°E
0.2±0.1km
53
1±0.5km
54
-3±1km
55
-2±1km
56
-7±4km
57
1.4±0.5km
58
-1.1±0.5km
59
≥-5±2km
60
≥-3±1.5km
61
≥-2±1km
62
-75±35km
63
-3.5±1.0km
64
-1.2±0.6km
65
-6±3km
67
-17±7km
68
≥-3±1.5km
66
≥-7±4.5km
69
-1±2km
47
-8.5±2km
48
-35±7 km
49
-3±1km
50
-10±4km
51
-25km
52
-3±1.5km
46
-7±3km
45
>-2km
44
-16±5km
43
>-10km
42
-12±3km
41
-8.5±3km
40
>-10km
39
>-12km
38

Figure 4

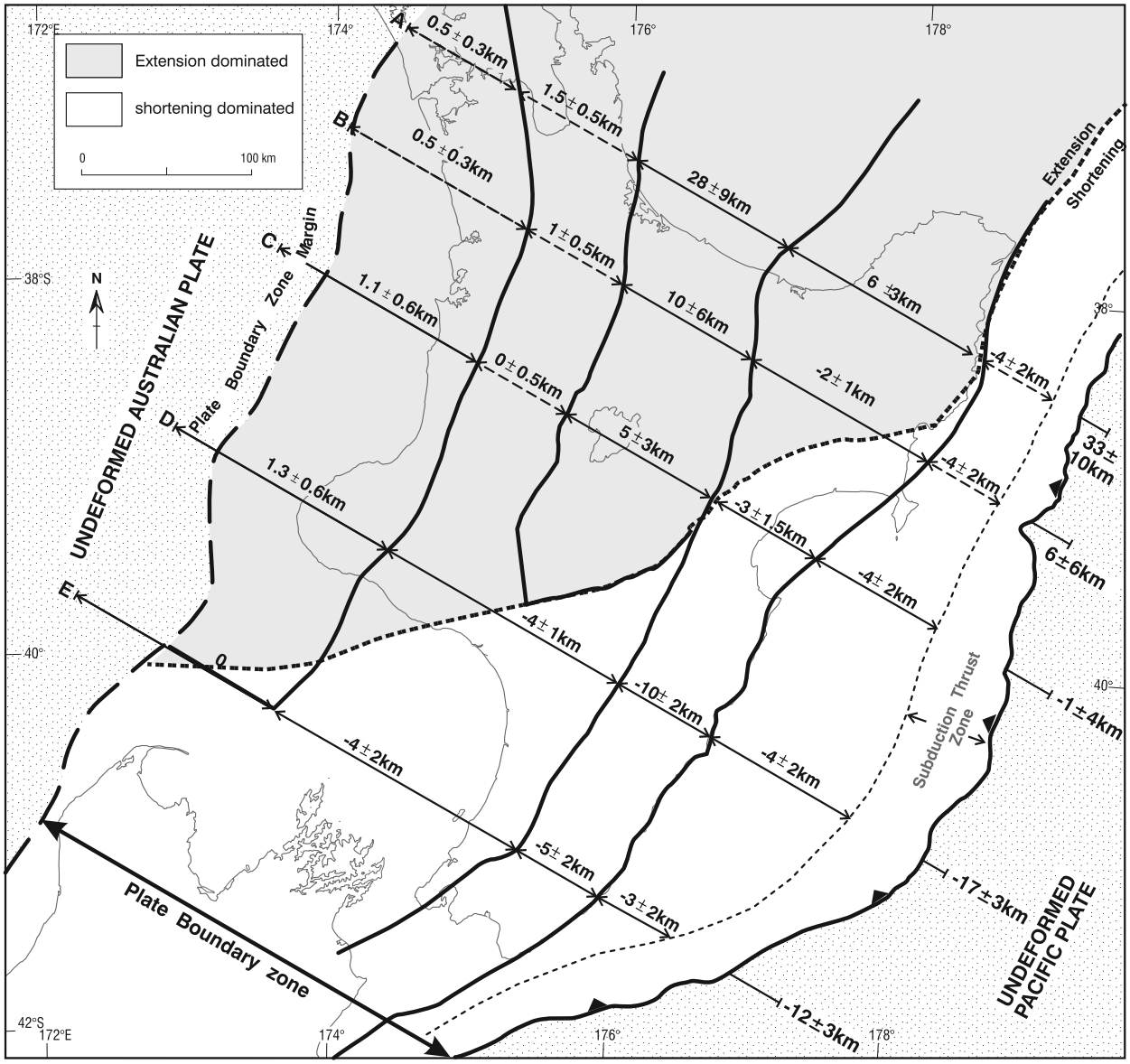

Figure 5. Map of the locations and strain estimates during the last ~5 Ma for five plate boundary profiles across the Hikurangi Margin. Strain profiles from Figure 3 were used to derive strain estimates along each transect. To aid the determination of strains along each transect the map is divided into five subareas. Total strain is indicated on the right-hand end of each profile. Regions of the plate boundary dominated by extension and shortening are differentiated.

tent with a northward thinning of the crust from 35 km (south of the Taupo Rift) to 20 km at Raukumara Peninsula [e.g., *Reyners et al.*, 1999, 2006]. On profile D average shortening rates since 5 Ma in the overriding plate are 3–4 mm/year (Figure 5). The total shortening and shortening rates in the upper plate are considerably less than the total plate convergence and the convergence rates for the margin at the latitude of profile D (ca. 170 km for 34 mm/year over 5 Myr), from which it can be argued that only a small proportion of plate convergence (~10%) was transmitted into the upper plate.

Figure 4. Strain map for Miocene structures. Strain profiles indicate margin-normal shortening (inward directed arrows and negative values) and extension (outward directed arrows and positive values). Shading in the North Island shows the extent of Mesozoic basement (dark grey), post-Cretaceous to Miocene (light grey) and post-Miocene (white) rocks. For description of data used to estimate strains in profiles, refer to website http://www.gns.cri.nz/research/basindynamics/strainprofiledata.html.

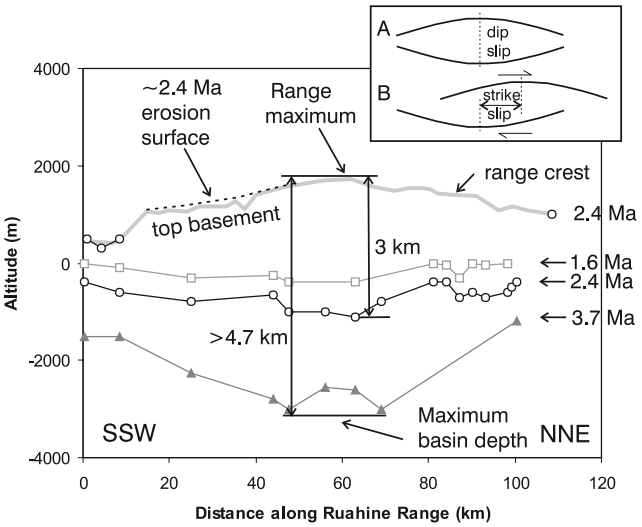

Figure 6. Horizon separation diagram showing tectonic vertical separations along the North Island Fault System in the central North Island. West of the faults in their uplifted hanging walls, the altitude of the range crest is plotted against distance northeast (~030°) of the Manawatu Gorge (see Figure 7 for location). The range crest comprises basement and scattered outcrops of 2.4-Ma strata, which rest directly on basement, and is assumed to provide a proxy for the 2.4-Ma horizon. The altitude of 1.6-, 2.4- and 3.7-Ma strata measured in the footwall of the North Island Fault System from 15–20 km east of the range crest are also shown. Range Crest topography is from spot heights on New Zealand 1:250,000, 262 Topomap series and the location of the Pliocene erosion surface from *Melhuish* [1990]. Altitudes of 2.4-Ma strata on the range crest are from mapping [*Melhuish*, 1990; *Lee and Begg*, 2002]. Altitudes of strata east of the faults are from seismic reflection data [*Melhuish*, 1990; *Beanland et al.*, 1998] and geological cross sections constructed normal to the faults using geological maps [*Erdman and Kelsey*, 1992; *Nicol and Beavan*, 2003]. Inset A, schematic horizon separation diagram for an ideal dip-slip fault [e.g., *Barnett et al.*, 1987]. Inset B, separation diagram from A transformed by post dip-slip right-lateral strike-slip.

The remainder of relative plate motion has been accommodated by displacement on the subduction thrust [*Nicol and Beavan*, 2003]. The proportion of plate convergence accommodated on the subduction thrust is highest in the northern margin (for example, profile A), where contemporary GPS and seismicity indicate that, beneath the North Island, the plate interface is experiencing stable sliding [*Reyners*, 1998; *Wallace et al.*, 2004]. Extension and associated contemporary clockwise rotation of the upper plate on Raukumara Peninsula results in a slip on the subduction thrust that exceeds the rate of plate convergence by 10–20 mm/year [*Wallace et al.*, 2004].

2.2. Miocene Deformation

[14] The best exposures of Miocene structures in the North Island occur along its east coast. These structures are dominated by superposed thrust sheets subparallel to bedding [e.g., *Chanier and Ferriere*, 1989, 1991] (profiles 38 and 39, Figure 4) and imbricate thrusts systems [e.g., *Pettinga*, 1982; *Barnes et al.*, 2002] (profiles 42–44, 46–48, Figure 4). Thrusts accommodate NW-SE contraction and are, in many cases, early Miocene (ca. 18–24 Ma) in age, having commenced movement during the onset of rapid subduction [*Chanier and Ferriere*, 1989, 1991; *Chanier*, 1991; *Rait et al.*, 1991; *Lee and Begg*, 2002; *Field et al.*, 1997; *Mazengarb and Speden*, 2000; *Barnes et al.*, 2002] (see also Figure 2a, particularly beneath the Gisborne-2 well). Early Miocene thrusting is present along the entire length of the Hikurangi Margin, suggesting that subduction had reached its present southern limit no later than 18 Ma [*Walcott*, 1984a; *Rait et al.*, 1991].

[15] Shortening of the upper plate accrued in response to plate convergence throughout the Miocene, although it appears that the rates of deformation varied temporally and spatially. In addition to the margin-wide early Miocene deformational event, periods of accelerated upper plate deformation may also have occurred in the middle (ca. 11–14 Ma) and late (ca. 5–7 Ma) Miocene [*Field et al.*, 1997; *Chanier et al.*, 1999; *Kamp*, 1999; *Nicol et al.*, 2002]. Accelerated deformation in the middle and late Miocene may indicate increases in the efficiency with which displacement was transferred from the subduction thrust into the upper plate rather than changes in the relative plate motion vector [*Nicol et al.*, 2002].

[16] Restored cross sections indicate an eastward temporal migration of deformation in the upper plate east of the North Island (Figure 8). In the early Miocene the locus of deformation on Figure 8 was concentrated in the western 80 km of the cross section, while structures in the easternmost part of the section are inferred to be post-Miocene (for example, compare ~16- and ~1.5-Ma restorations). This migration appears to have been associated with a ca. 40 km eastward shift in the surface trace of the subduction thrust during the late Miocene (Figure 8). *Barnes and Mercier de Lépinay* [1997] documented an eastward shift in the subduction thrust of similar magnitude within the last million years 130 km south of Figure 8 (see Figure 7 for location). Episodic and eastward propagation of the subduction thrust by 20–40 km into 2- to 3-km-thick sediments on the incoming plate appears to be an important mode of material transfer into the accretionary wedge. The resultant low taper angle on the wedge supports the view that the basal friction on the subduction thrust is low [cf. *Gutscher et al.*, 1998].

[17] In the Raukumara Peninsula, folded and faulted strata recorded early Miocene NE-SW shortening associated with obduction of the east coast allochthon from the subducting Pacific Plate [*Rait*, 2000]. The difference in the direction of contraction between Raukumara Peninsula and regions to the south (i.e., in the areas of profiles 38–51) arises in part because of a clockwise rotation of the Hikurangi Margin from northern Hawkes Bay southward (see section 4 for further discussion). Thrusting is accompanied by minor middle Miocene and younger extension of Raukumara Peninsula and of the region east of the axial ranges [e.g., *Cashman and Kelsey*, 1990; *Field et al.*, 1997;

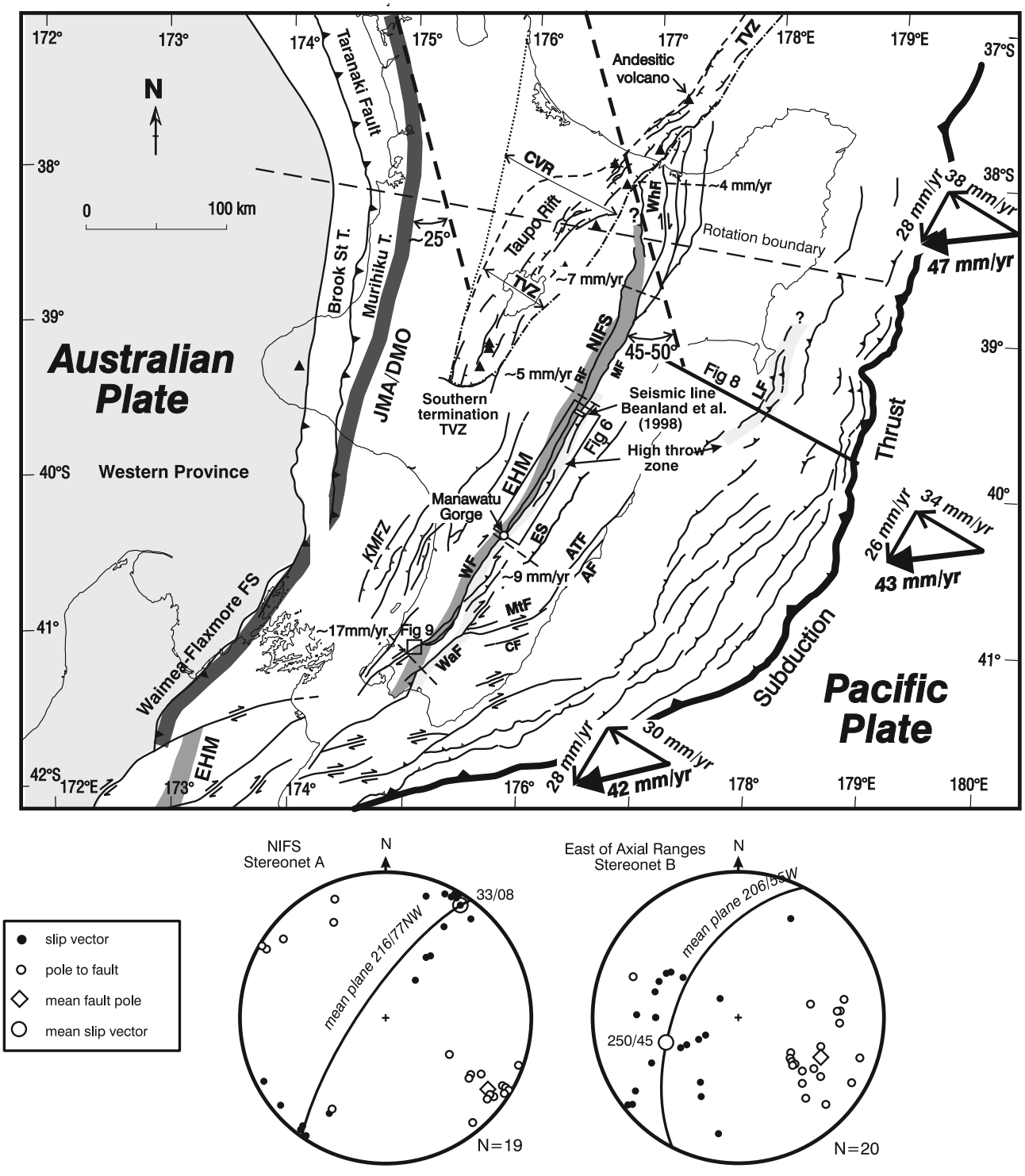
Australian Plate
Pacific Plate
Western Province
Taranaki Fault
Brook St T.
Murihiku T.
JMA/DMO
Andesitic volcano
TVZ
CVR
Taupo Rift
WhF
Rotation boundary
~4 mm/yr
~7 mm/yr
~25°
45-50°
NIFS
RF
MF
LF
Fig 8
Seismic line Beanland et al. (1998)
Fig 6
High throw zone
Thrust
Southern termination TVZ
~5 mm/yr
EHM
Manawatu Gorge
KMFZ
WF
ES
ATF
AF
~9 mm/yr
MtF
CF
WaF
~17mm/yr
Fig 9
Waimea-Flaxmore FS
Subduction
28 mm/yr
38 mm/yr
47 mm/yr
26 mm/yr
34 mm/yr
43 mm/yr
30 mm/yr
42 mm/yr
0
100 km
172°
173°
174°
175°
176°
177°
178°E
179°E
180°E
37°S
38°S
38°
39°
40°S
40°
41°
41°S
42°S
172°E

slip vector
pole to fault
mean fault pole
mean slip vector
NIFS Stereonet A
N
33/08
mean plane 216/77NW
N=19
East of Axial Ranges Stereonet B
N
mean plane 206/55W
250/45
N=20

Figure 7

Mazengarb and Speden, 2000; *Barnes et al.*, 2002; *Barnes and Nicol*, 2004]. These normal faults may have formed because of tectonic erosion, oversteepening and gravitational collapse of the accretionary wedge [*Chanier et al.*, 1999], and in response to sediment underplating beneath, and associated uplift of, the Raukumara Peninsula [*Walcott*, 1987; *Reyners and McGinty*, 1999; *Upton et al.*, 2003].

[18] Miocene normal and reverse faults are present on the western side of the plate boundary zone. Within the Taranaki Basin, mid-late Miocene extension is small (<1.5 km, profiles 53 and 54) and gives way to contraction of the same age south of profile 57 (Figure 4). The reverse Taranaki Fault and its southern continuation, the Waimea-Flaxmore Fault System (see Figure 4 for location), dominate Miocene deformation on the western side of the plate boundary zone. Like many faults in the North Island these structures are parallel to the trend of Mesozoic basement terranes (compare Figures 1 and 7). This parallelism suggests that many post-Oligocene Faults (including the Taranaki Fault) occupy preexisting planes of weakness within basement (for example, terrane boundaries, stratigraphic contacts, and faults). The Taranaki Fault is a crustal scale thrust antithetic to the subduction thrust. The fault dips eastward at 25°–45° and forms the eastern boundary of the Taranaki Basin (Figure 7), which contains a sedimentary succession up to about 8 km thick [*Thrasher et al.*, 1995; *King and Thrasher*, 1996; *Nicol et al.*, 2004] (Figure 2b). The Taranaki Fault appears to have been active from the middle Eocene onward (i.e., 40–45 Ma), with accelerated rates of movement during the early to middle Miocene [*King and Thrasher*, 1996; *Nicol et al.*, 2004]. Total Miocene throw on this structure of $\geq$4 km is, for all but the northern most profile (profile 55, see Figure 4), a minimum because early Miocene and older strata were either not deposited on or, more likely, eroded from its hanging wall. In the northern South Island, Murihiku, Brook Street, and Dun Mountain Ophiolite (marked by the Junction Magnetic Anomaly) basement terranes are contained within the 10- to 15-km-wide Waimea-Flaxmore Fault Zone and overthrust western province batholiths [*Rattenbury et al.*, 1998]. The minimum throw of the Waimea-Flaxmore Fault since the Oligocene is 3–4 km [*Rattenbury et al.*, 1998], with shortening in a NW-SE direction [*Pettinga and Wise*, 1994].

[19] Total shortening of 75 ± 35 km across the Taranaki and Wanganui basins (including the Taranaki Fault System) is estimated from a deep crustal seismic line for crustal thickening from ca. 25 to 40 km [e.g., *Holt and Stern*, 1994] (profile 63, Figure 4, see Web site http://www.gns.cri.nz/research/basindynamics/strainprofiledata.html for shortening estimate derivation). Although our estimate of shortening is comparable to the 70 ± 30 km of *Stern et al.* [2006], it cannot be confirmed by the analysis of deformation of Miocene and older strata, which have been entirely removed from the hanging wall of the Taranaki Fault System at the location of the deep crustal seismic line. A Miocene age for this shortening is inferred from the Miocene or older timing of shortening across the Taranaki Fault at the latitude of profile 63 [*Nicol et al.*, 2004] and from the post-Oligocene age of thrusting and associated WNW-ESE shortening in the northern South Island (>7 ± 4.5 km, profile 69, Figure 4) [*Nicol and Campbell*, 1990]. Miocene shortening in the Taranaki and Wanganui basins is consistent with the timing and amount of shortening per kilometer of line length ($\sim$1-km shortening per 4-km predeformation line length) east of the axial ranges. Aggregating 75 ± 35-km shortening across the Taranaki and Wanganui basins and 40 ± 10 km from east of the axial ranges (for example, sum profiles 41, 43, 44, and 45 or sum profiles 41 and 49) produces 115 ± 45-km Miocene shortening normal to the margin and across the entire plate boundary zone at a latitude of 39°–41°S. The total Miocene convergence between the Australian and Pacific plates at this location was ca. 670 km (i.e., an average of 35 km/Myr [*Cande and Stock*, 2004] for the 19-Myr duration of the Miocene), with 10–25% of the total convergence inferred to have been accommodated by shortening observed in the upper plate (i.e., 115 ± 45 km) at average rates for the Miocene of about 4–8 mm/year. As shortening near to the subduction thrust may be interplate (as has been suggested for the last 5 Myr), this estimate of the average Miocene shortening rate is inferred to be a maximum for the upper plate.

3. Strike-Slip Faulting

[20] Ever since Wellman demonstrated 480 km of strike separation along the Alpine Fault over 50 years ago [*Benson*, 1952], workers have been proposing, and presenting evidence for, strike-slip faults with large right-lateral displacements in the North Island [e.g., *Kingma*, 1958; *Ballance*, 1976; *Cole*, 1986; *Lamb*, 1988; *Cashman et al.*, 1992; *Beu*,

Figure 7. Map of generalized geology of basement rocks in the Hikurangi Margin (modified after the work of *Mortimer* [1995]). Strike-slip (asymmetric arrows) and reverse (teeth) faults from Figure 1. Equal-area lower hemisphere projections of fault planes and slip vectors for the North Island Fault System (stereonet, A) and the onshore region east of the axial ranges (stereonet, B). Slip data from offset geomorphological markers (for example, abandoned streams, ridges, and terrace margins) and slickenside striations on fault surfaces [*Raub*, 1985; *Grapes and Wellman*, 1988; *Berryman*, 1990; *Berryman and Beanland*, 1991; *Erdman and Kelsey*, 1992; *Van Dissen et al.*, 1992; *Beanland*, 1995; *Kelsey et al.*, 1995, 1998; *Van Dissen and Berryman*, 1996; this study]. Cumulative slip rates across the North Island Fault System (including the eastern strand) from *Beanland* [1995], *Schermer et al.* [2004], and *Mouslopoulou et al.* [2007], with the southernmost value excluding 4 mm/year inferred for the Wairau Fault offshore west of the North Island. Locations of Figure 9 indicated. Abbreviations: JMA, Junction Magnetic Anomaly; DMO, Dun Mountain Ophiolite; EHM, Esk Head Mélange; T, terrane; TVZ, Taupo Volcanic Zone; CVR, Central Volcanic Zone; ES, eastern strand of North Island Fault System; ATF, Adams-Timui Fault; AF, Akito Fault; CF, Carterton Fault; MF, Masterton Fault; MF, Mohaka Fault; RF, Ruahine Fault; WaF, Wairarapa Fault; WF, Wellington Fault; WhF, Whakatane Fault.

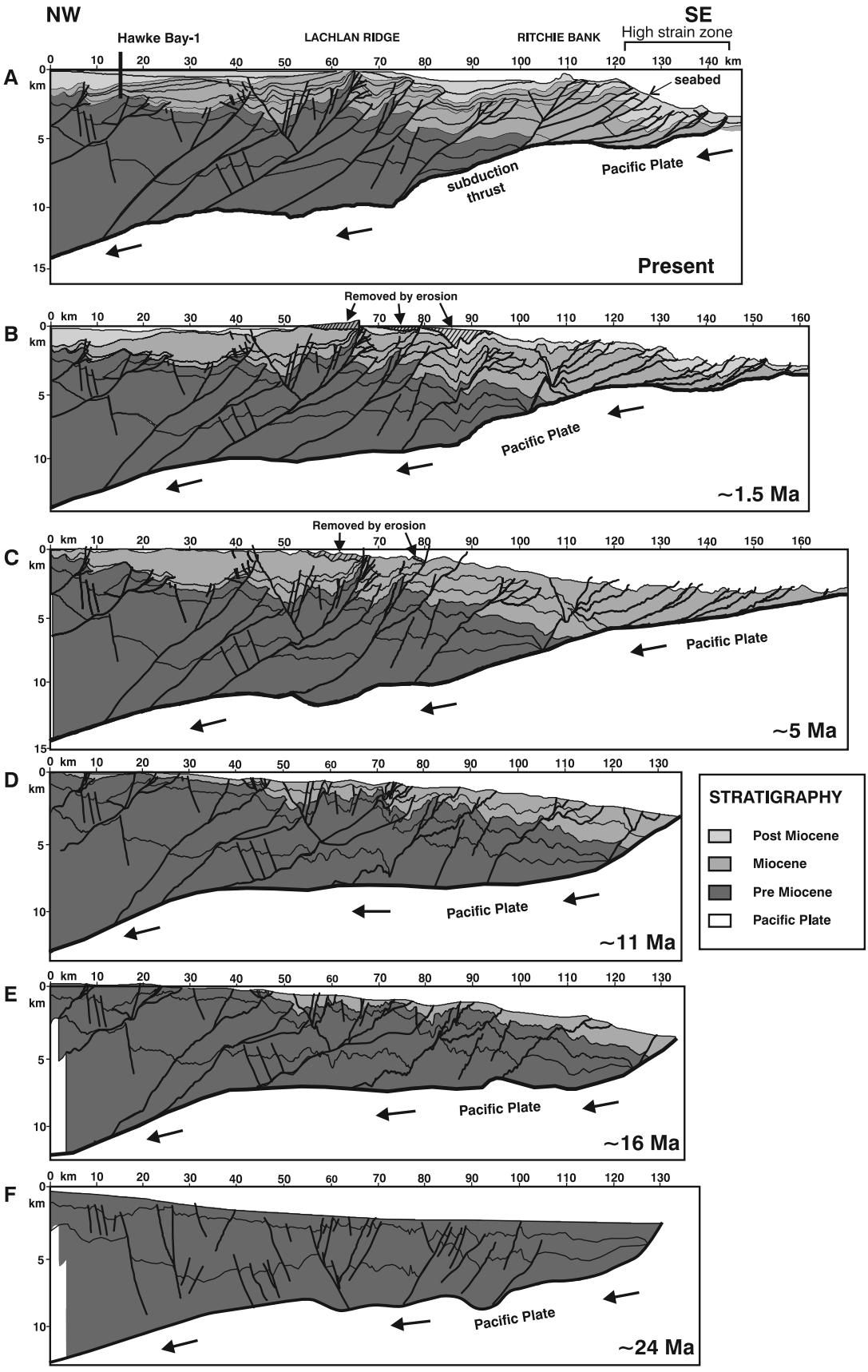
NW
SE
Hawke Bay-1
LACHLAN RIDGE
RITCHIE BANK
High strain zone
A
seabed
subduction thrust
Pacific Plate
Present
Removed by erosion
B
Pacific Plate
~1.5 Ma
Removed by erosion
C
Pacific Plate
~5 Ma
D
Pacific Plate
~11 Ma
STRATIGRAPHY
Post Miocene
Miocene
Pre Miocene
Pacific Plate
E
Pacific Plate
~16 Ma
F
Pacific Plate
~24 Ma

Figure 8

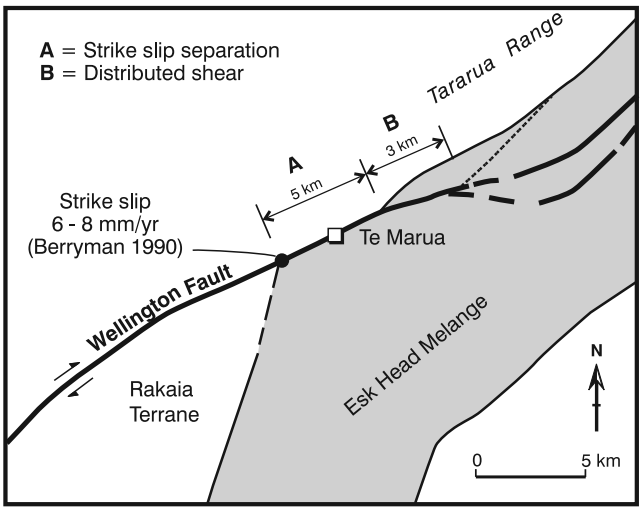

Figure 9. Map of the Wellington Fault at Te Marua showing a total of up to 8-km strike separation and possible distributed shear along the fault (data from *Begg and Mazengarb* [1996]). See Figure 7 for location.

1995; *Mortimer*, 1995; *Delteil et al.*, 1996]. The most extreme strike-slip models proposed require in excess of 300-km right-lateral displacement on faults within the Hikurangi Margin since the start of the Miocene (see review of *King*, 2000, Figure 3). As the strike of faults is typically subparallel to the trend of Mesozoic terrane boundaries, few piercing points in bedrock provide unequivocal measures of strike-slip and models for large (for example, >50 km) strike-slip remain controversial.

[21] The most compelling evidence for strike-slip is on the principal faults of the active North Island Fault System (Figure 7). These faults, which include the Wellington, Wairarapa, Mohaka, Ruahine, and Whakatane faults (see Figure 7), are steeply dipping (mean 77°W, Figure 7, stereonet A) and displace Late Quaternary (<50 ka) landforms (for example, terrace risers, ridges and abandoned stream channels) by tens of meters [*Beanland and Berryman*, 1987; *Raub et al.*, 1987; *Berryman and Beanland*, 1988; *Grapes*, 1991; *Erdman and Kelsey*, 1992; *Beanland*, 1995; *Van Dissen and Berryman*, 1996; *Langridge et al.*, 2005]. Slip vectors principally measured from displaced landforms indicate that these faults also carry small components of normal or reverse displacement (Figure 7). Displaced landforms and slickenside striations on faults onshore and east of the axial ranges indicate mainly reverse dip-slip with subordinate right-lateral strike-slip, which is mainly confined to the eastern strand of the North Island Fault System (see ES and stereonet B on Figure 7). Late Quaternary slip rates in the North Island Fault System increase southward from 4 mm/year at the north coast to 18 mm/year in the south near Wellington (Figure 7) [e.g., *Beanland*, 1995; *Mouslopoulou et al.*, 2007].

[22] Geological mapping of the southern North Island [*Lee and Begg*, 2002] together with seismic reflection profiles and swath bathymetry from offshore of this region [*Collot et al.*, 1996; *Barnes and Mercier de Lépinay*, 1997; *Barnes and Audru*, 1999] and modeling of GPS velocities [*Wallace et al.*, 2004] also indicate some strike-slip faulting outside the North Island Fault System (for example, Masterton and Carterton faults, see Figure 7). The southward increase of strike-slip in the southern ~100 km of the North Island is due, in part, to an ~2–3 mm/year southward increase in the magnitude of the margin-parallel component of relative plate motion (Figure 7).

[23] Faults in the North Island Fault System do not appear to have accrued substantial total strike-slip (for example, >20 km). To the south, the Wellington Fault produces an apparent right-lateral separation of about 5 km on the western boundary of the Esk Head Mélange [*Begg and Mazengarb*, 1996], a basement terrane of Mesozoic age (Figure 9). The Mesozoic tectonic fabric within the mélange is steep (>60°), and its along-fault separation gives a first-order estimate of strike-slip. In addition to fault displacement, up to 3 km of distributed off-fault right-lateral displacement may have accrued north of the fault, producing a total strike-slip of ca. 5–8 km (Figure 9). This strike-slip is comparable to the 7 ± 1-km right-lateral displacement, inferred from the deflection of the main rivers that cross the Wellington Fault ~5–50 km north of Figure 9 [*Berryman et al.*, 2002].

[24] Total strike-slip on the Wellington Fault is consistent with the inferred lateral displacement on the Mohaka and Ruahine faults. The horizon separation diagram in Figure 6 is indistinguishable from those observed on dip-slip faults [e.g., *Chapman et al.*, 1978; *Barnett et al.*, 1987] (Figure 6, inset A). As the strike-slip is inferred to postdate dip-slip on these faults [*Kelsey et al.*, 1995], >20-km right-lateral strike-slip would be expected to displace the point of maximum range altitude NNE of the greatest basin depth (for example, Figure 6 inset B). Figure 6 shows no such displacement, and we infer that strike-slip on the Mohaka and Ruahine faults in the last 2.4–3.7 Myr could have been no greater than the lateral resolution of the horizon locations, i.e., about 20 km. These values of strike-slip are

Figure 8. Cross sections derived from seismic line CM05-01, Hawkes Bay, structurally balanced using 2DMove software to backstrip fault displacements, unfold strata, and decompact sediments. Structural restorations of the interpreted (a) cross section are presented for (b) top Pliocene, (c) top Miocene, (d) top middle Miocene, (e) top early Miocene, and (f) top Paleogene horizons. Selected horizons were traced across much, or all, of the section and record deformation at approximately equal time increments over the last 24 Myr. Stratigraphy in the section from Hawke Bay-1 well (location shown) and seabed outcrop [*Barnes et al.*, 2002]. The restorations are regarded as first order and have been vertically exaggerated approximately three times to provide improved definition of the structure and stratigraphy. Refer to the work of *Nicol and Uruski* [2005] for further details of the restoration. See Figure 7 for location.

Table 1. Paleomagnetic Rotation Data, North Island, New Zealand

Sample Number	Originators Sample Name	Location[a]		Sample Age[b]		Rotation[c] (°)	Reference[d]
		Easting	Northing	NZ Stage	Ma		
1	BENNEY DALE	2718057	6295843	Ld	26.2 ± 1.1	54.5 ± 10	1
2	BEXLEY STN 2	2660712	6282832	l Lwh	32.6 ± 1.8	58 ± 17	1
3	PONGANUI RD	2672230	6421799	l Lwh	32.6 ± 1.8	28.8 ± 7	1
4	HB1	2911712	6267389	l Tt	9.9 ± 1.1	27.8 ± 12	2
5	HK1	2966800	6387900	Lw-Po	21.9 ± 2.9	−6.2 ± 7	3
6	RAURIMU	2716640	6229577	Lw-Po	21.9 ± 2.9	12.3 ± 7	1
7	TAUMARUNUI	2699726	6249170	Lw-Po	21.9 ± 2.9	29.6 ± 18	1
8	PT4	2920718	6270272	Lwh-Lw	28 ± 6.3	199 ± 21	2
9	TA3	2978600	6368500	Pl	17.5 ± 1.5	21 ± 5	4
10	TA4	2978400	6368700	Pl	17.5 ± 1.5	9 ± 6	4
11	TA6	2979800	6372900	base Pl	19 ± 0.5	4 ± 6	4
12	MA1	2968100	6319800	Pl	17.5 ± 1.5	9 ± 4	4
13	TA7	2979500	6365500	Pl-Sc	17 ± 2	10 ± 4	4
14	MK1	2917700	6252750	Pl-Sc	17 ± 2	62.7 ± 10	3
15	MK2	2917500	6252700	Pl-Sc	17 ± 2	44.9 ± 16	3
16	PT3	2920314	6271124	Pl-Sc	17 ± 2	179 ± 23	2
17	HK2	2971700	6387700	Po	20.4 ± 1.4	5.3 ± 11	3
18	HK3	2972700	6387700	Po	20.4 ± 1.4	19.3 ± 13	3
19	JK4	971800	6387700	Po	20.4 ± 1.4	22 ± 4	3
20	TA2	2974900	6378200	Po	20.4 ± 1.4	23 ± 8	4
21	RK	2911770	6298820	Po	20.4 ± 1.4	18 ± 9	5
22	HR3	2906150	6275900	Sc-Sw	13.5 ± 2.5	130 ± 10	3
23	TP1	2958000	6271000	Sc-Sw	13.5 ± 2.5	87.3 ± 12	2
24	AV1	2914910	6269664	Sc-Sw	13.5 ± 2.5	19.2 ± 6	2
25	HR1	2920400	6276000	Sl-Sw	13 ± 2	44.5 ± 8	3
26	HR2	2919700	6273600	Sl-Sw	13 ± 2	94.3 ± 25	3
27	WK1	2866400	6266800	Sl-Sw	13 ± 2	69.7 ± 30	3
28	PT1	2919863	6273276	Sl-Sw	13 ± 2	44.6 ± 16	2
29	MW1	2913064	6269092	Sl-Sw	13 ± 2	39.5 ± 52	2
30	HG1	2913064	6270873	Sw-Tt	9.9 ± 3.4	43.6 ± 12	2
31	WV1	2948913	6283778	base Wo	5.3 ± 0.3	4.7 ± 10	2
32	TB1	2973000	6293000	Tt	8.8 ± 2.2	8.9 ± 8.9	2
33	KA1	2948000	6267000	Tt	8.8 ± 2.2	56.3 ± 3	2
34	HINEKURA	2731500	5986300	uTt	7.7 ± 1.2	30.1 ± 3.4	6
35	MK3	2914000	6238000		15 ± 1	94.7 ± 27	3
36	MK4	290500	6246000		4 ± 0.5	21.7 ± 12	3
37	MK5	2905600	6245500		5 ± 0.5	40.5 ± 10	3
38	MK6	2907000	6245000		6 ± 0.5	28.8 ± 11	3
39	MK7	2914000	6244000		10 ± 1[e]	47.2 ± 4	7
40	MK8	2912000	6244000		9 ± 1[e]	39.7 ± 3	7
41	MK9	2910000	6244000		8 ± 1[e]	41.2 ± 5	7
42	MK10	2908500	6245000		6 ± 0.5[e]	21.7 ± 11	7
43	WH1	2875664	6232262		2 ± 0.5[e]	17.4 ± 5	7
44	WANGANUI RIVER	2687300	6184100		2.5 ± 0.1[e]	3.9 ± 3.9	8
45	TURAKINA RIVER	2725600	6164000		2.5 ± 0.1[e]	9 ± 2	8
46	RANGITIKEI RIVER	2756900	6156900		2.5 ± 0.1[e]	15.7 ± 3.1	8
47	SOUTH WAIRARAPA	?	?	?	2.2 ± 0.2	−4 ± 6	9
49	MANAWATU STRAIT	2747500	6098500	l Wn	2.2 ± 0.2	4 ± 2	10

[a]Grid references in New Zealand Map Grid Projection (1949 Geodetic Datum).

[b]Numerical ages based mainly on recent geological mapping and paleontological data [e.g., *Begg and Johnston*, 2002; *Mazengarb and Speden*, 2000; *Lee and Begg*, 2002]. Age midpoint of quoted NZ stage using timescale of *Cooper* [2004] with uncertainties equal to time range of stage(s).

[c]Declination of remanent magnetism (relative to True North) after cleaning (thermal or alternating field) and bed dip correction. Uncertainties are given to the 95% confidence level.

[d]1, *Mumme and Walcott* [1985]; 2, *Thornley* [1996]; 3, Walcott and Mumme [1982]; 4, *Mumme et al.* [1989]; 5, *Rowan et al.* [2005]; 6, *Walcott et al.* [1981]; 7, *Wright and Walcott* [1986]; 8, *Wilson and McGuire* [1995]; 9, *Lamb* [1988]; 10, *Beanland* [1995].

[e]Age assigned from magnetostratigraphy.

consistent with a seismic reflection line (see Figure 7 for location), which crosses the Mohaka Fault and shows an apparent vertical displacement of an ~2.4-Ma limestone of ca. 20–30 m [*Beanland et al.*, 1998]. Given the 10:1 horizontal to vertical ratio of Late Quaternary slip [*Beanland*, 1995], the apparent throw could have been produced by as little as 200–300 m of strike-slip since the late Pliocene. Collectively, the available data lead us to concur with *Beanland* [1995] in suggesting that the total strike-slip in the North Island Fault System is small (for example, <20 km).

[25] Strike-slip displacement of more than several kilometers has not been unequivocally demonstrated on faults east or west of the North Island Fault System. To the west of the axial ranges, the geometries of faults imaged in seismic reflection profiles of good quality are not consistent with significant strike-slip, particularly in the last 5 Myr [*Anderton*, 1981; *King and Thrasher*, 1996]. East of the ranges strike-slip displacements of 16–350 km have been postulated for the Poukawa-Oruawharo Fault Zone (ES on Figure 7) [*Kingma*, 1958; *Cashman et al.*, 1992; *Beu*, 1995] and the Adams-Tinui and Akito fault zones [*Delteil et al.*, 1996] since the start of the Miocene (Figure 7 for fault locations). Recent geological mapping and trenching of the Poukawa Fault Zone indicates predominately reverse dip-slip [*Kelsey et al.*, 1998], while the geometries and kinematics of the Adams-Tinui and Akito faults support an imbricate thrust stack model [*Pettinga*, 1982; *Chanier*, 1991; *Lewis and Pettinga*, 1993; *Rait*, 1997]. Strike-slip in excess of 200–300 km [e.g., *Delteil et al.*, 1996] would be expected on long (for example, 300–600 km) continuous and relatively unsegmented faults [*Wesnousky*, 1988]. The preponderance of short (<50–100 km), segmented, and discontinuous faults, which, in some cases, bound basement outcrop (Figure 1), together with the lack of unequivocal strike-slip kinematic indicators lead us to conclude that strike-slip has been minimal (for example, <10 km) on faults east of the axial ranges.

4. Vertical-Axis Rotations

[26] Over the last three decades the study of declinations of primary magnetism in sedimentary rocks ranging up to ca. 32 Ma in age has provided a basis for the recognition of vertical-axis rotations of the crust in New Zealand [e.g., *Kennett and Watkins*, 1974; *Mumme and Walcott*, 1985; *Wright and Walcott*, 1986; *Lamb*, 1988; *Walcott*, 1989; *Roberts*, 1992, 1995; *Wilson and McGuire*, 1995; *Thornley*, 1996; *Little and Roberts*, 1997; *Rowan et al.*, 2005]. Modeling of geodetic velocities [*Walcott*, 1984b; *Beavan and Haines*, 2001; *Wallace et al.*, 2004] and Late Quaternary fault slip rates [*Beanland and Haines*, 1998] indicates that these rotations continue to the present-day. We use paleomagnetic data in combination with strain gradients along the margin, bending of Mesozoic terranes and GPS velocities to constrain rotations about vertical axes within the Hikurangi Margin.

[27] Paleomagnetic data for the North Island from a number of sources are summarized in Table 1 and presented in Figures 10 and 11. These data have been corrected for the tilt of strata and for secular variation (refer to original publications for further discussion). The rocks are typically weakly magnetized with low signal-to-noise ratios, which are reflected in the high uncertainties of many of the declinations (for example, $\leq\pm100\%$). Measurement errors may result in significant variations of rotations for samples on the same local structure and within rocks of similar age (for example, compare samples 26 and 28, Table 1). In addition, some rotations may also be influenced by their proximity to local structure. Extreme paleomagnetic rotations recorded by samples 8 and 16 (Table 1) close to the Waerengaokuri Fault (Figure 10) may, for example, have been induced by locally high shear strains [*Thornley*, 1996]. Although some paleomagnetic rotations may have significant errors [cf. *Rowan et al.*, 2005] or vary locally due to tectonics, the reproducibility of the general results indicates that first-order conclusions based on these data are probably robust.

[28] The samples are unevenly distributed in space with most being from the northern part of Hikurangi Margin (Figure 10). Many of the samples were collected to constrain the location of a rotation boundary near Gisborne [e.g., *Walcott*, 1989; *Thornley*, 1996; Walcott and Mumme, 1982]. This boundary separates rocks of the Raukumara Domain with mainly 0°–20° clockwise rotations, from strata to the south in the Wairoa Domain that are commonly rotated clockwise by up to 60°–90° (Figures 10 and 11). The boundary is not coincident with known faults, and the high strains required at the boundary are inferred to be distributed across the zone [*Thornley*, 1996]. The westward projection of this rotational boundary broadly coincides with ca. 25° changes in the trends of the North Island Fault System, Taranaki Fault, and Junction Magnetic Anomaly/Dun Mountain Ophiolite (Figure 7). This coincidence provides a measure of geological support for the existence of the rotation boundary. However, the geodetic velocity field [*Walcott*, 1989; *Beavan and Haines*, 2001; *Wallace et al.*, 2004] and modeling of Late Quaternary fault displacements [*Beanland and Haines*, 1998] show the entire eastern North Island to be rotating at a rate of ~3°/Myr (with respect to stable Australian Plate), with no difference between Raukumara and Wairoa domains. The rotational boundary (Figure 7) may have been abandoned 1–2 Myr ago [*Nicol and Wallace*, 2007] when rifting and volcanism commenced in the Taupo Volcanic Zone [*Wilson et al.*, 1995].

[29] In the Raukumara Domain the rates of clockwise vertical-axis rotation were about 1°/Myr since ca. 24 Ma (Figure 11), which is approximately equal to the bulk rates of clockwise rotation of the Australian Plate, as indicated by the polar wander path of *Idnurm* [1985]. Therefore, within the measurement uncertainties, the Raukumara Domain is unrotated with respect to the undeformed Australian Plate west of New Zealand.

[30] Rates of rotation for the last 10 Myr in the Wairoa Domain are typically in the range of 3°–5°/Myr (Figure 11). If the bulk clockwise rotation of the Australian Plate was about 1°/Myr, then, since 10 Ma, the Wairoa Domain rotated at about 2°–4°/Myr with respect to stable Australian Plate west of New Zealand. This estimate is consistent with previous interpretations of paleomagnetic data [e.g., Walcott and Mumme, 1982], the ~3°/Myr modeled from GPS velocities [*Wallace et al.*, 2004] and the ~3.5°/Myr required by the southward increase in shortening along the margin [*Nicol and Wallace*, 2007]. The clockwise rotations of the Hikurangi Margin relative to stable Australian Plate prior to 10 Ma are poorly constrained by the paleomagnetic data (Figure 11).

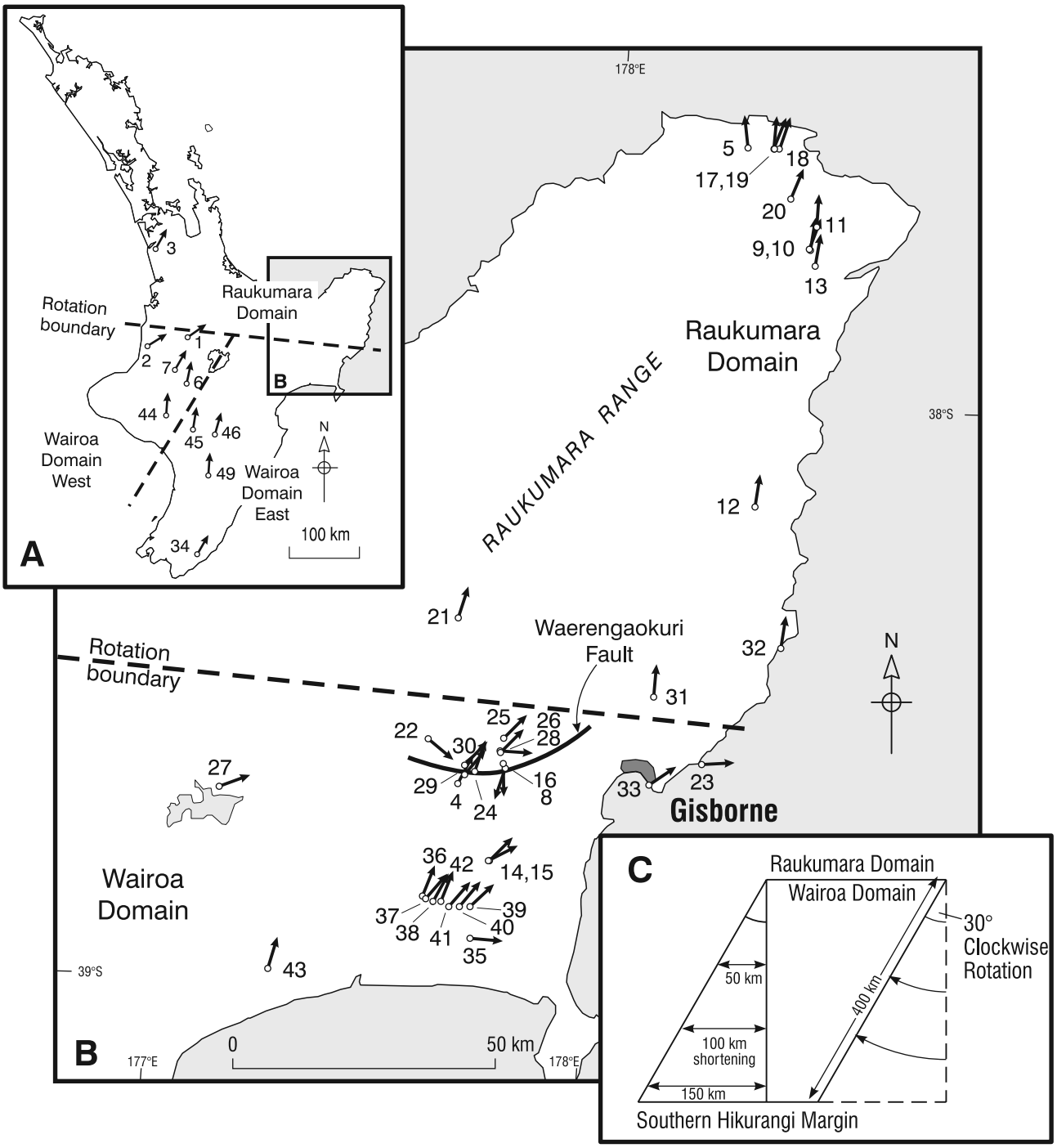

Figure 10. (a) Locations and declinations for paleomagnetic samples from the southern, western, and central North Island and (b) the northeast-east North Island. Absolute rotations about vertical axes (i.e., including bulk rotation of the Australian Plate) indicated by the angular divergence of each arrow from north. Sample numbers given in Table 1 are indicated. Rotational boundaries between the Wairoa and Raukumara domains (Figure 10a and 10b) and eastern and western Wairoa domain (Figure 10a) are shown. For further details of the data, refer to Table 1 and section 4. (c) Schematic diagram showing the southward increase in shortening across the Hikurangi Margin arising due to the 30° clockwise rotation.

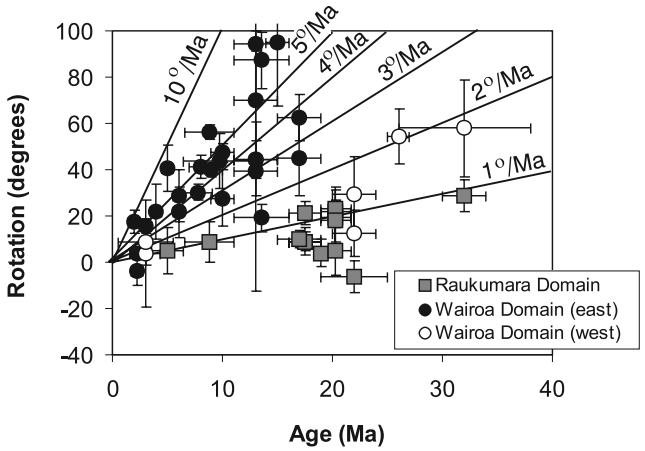

Figure 11. Plot of vertical-axis rotation versus paleomagnetic sample age for Tertiary strata. Positive rotations are clockwise and negative anticlockwise. Constant rotation rates of 1°–5°/Myr and 10°/Myr are indicated. Rukumara Domain (grey squares), Wairoa Domain west of the TVZ and KMFZ (open circles), and Wairoa Domain east of the TVZ and KMFZ (filled circles) are shown. Refer to Table 1 and section 4 in the text for further sample details.

[31] Late Miocene and younger rotation rates in the Wairoa Domain (relative to undeformed Australian Plate) decrease from about 3°/Myr east of the North Island Fault System to zero at the western margin of the plate boundary [*Wilson and McGuire*, 1995; *Wallace et al.*, 2004; *Nicol and Wallace*, 2007]. Decreases in rotation rates appear to occur principally across the North Island Fault System, the Taupo Rift, and the Kapiti-Manawatu Fault Zone (Figure 7). These decreases are consistent with the rotational block model of *Wallace et al.* [2004] and with the Pliocene-Pleistocene rotational model of *King and Thrasher* [1996] for the Taranaki Basin. Due in part to the westward decrease in rotation rates, paleomagnetic data from the west of the Taupo Rift and Kapiti-Manawatu Fault Zone (Wairoa Domain west) tend to plot on Figure 11 below the samples from further east. The westward decrease in the post middle Miocene rates of rotation are accompanied by a decrease of shortening rates in the same direction [*Nicol and Beavan*, 2003] and are consistent with the poles to these rotations (relative to a fixed Australian Plate) being located close to the western margin of the plate boundary zone (Figure 12) [*King and Thrasher*, 1996; *Beanland and Haines*, 1998; *Wallace et al.*, 2004]. The westward decrease in rotation rates is schematically illustrated in Figure 12 where hypothetical marker lines are progressively bent clockwise as they approach the subduction thrust by applying present rotation rates for 10 Myr. The eastward increase in rotations is achieved in two main steps located along the Taupo Rift to Kapiti-Manawatu Fault Zone and the North Island Fault System (Figure 12). These faults define the boundaries of three large crustal blocks within which the amount and rate of rotation are approximately constant. The resulting bending of the Australian Plate occurs about a vertical axis approximately positioned at the southern termination of subduction and coincident with the pole of rotation of the Australian Plate relative to a fixed Pacific Plate (open circle, Figure 12). Clockwise rotation and bending of the upper plate may arise in part because the change from subduction to continental collision at the southern termination of the margin applies a torque to the eastern North Island, which diminishes with increasing distance from the subducting plate [*Wallace et al.*, 2004]. Rotations may also have been enhanced by a slab rollback of the subducting Pacific Plate in the northern margin [*Walcott*, 1987].

[32] The late Miocene rates of rotation and their westward decrease may not have applied for the duration of subduction. Paleomagnetic data suggest rotation rates of 3°/Myr (relative to stable Australian Plate) for the last 10 Myr in the eastern Wairoa Domain (Figure 11), which would produce 30° rotation. The Junction Magnetic Anomaly/Dun Mountain Ophiolite swings clockwise ~25° across the Raukumara/Wairoa rotational boundary, in accord with the rotation of paleomagnetic samples 1 and 2 (Table 1). In the Wairoa Domain the Esk Head Melange (EHM) basement terrane trends 20°–25° clockwise of the Junction Magnetic Anomaly/Dun Mountain Ophiolite trend. If the divergence of these two trends is due principally to spatial variations in vertical-axis rotations, then the total clockwise rotation of the Esk Head Melange is ~45°–50°. Approximately 30° of this total rotation occurred during the last 10 Myr and, if the remaining ~15°–20° accrued since the onset of subduction at 24–30 Ma, the average rates of rotation (relative to stable Australian Plate) prior to 10 Ma would have been ~1°/Myr. A similar decrease in rotation rates has previously been inferred to have occurred at 5–10 Ma [*Walcott*, 1989; *Rowan et al.*, 2005]. This change in rate may have been accompanied by a change from the bending depicted in Figure 12 to approximately uniform rotation rates across the entire margin prior to 10 Ma. This inference is consistent with the 20°–25° finite rotation of the Junction Magnetic Anomaly/Dun Mountain Ophiolite, 10°–20° of which accrued prior to 10 Ma (i.e., 20°–25° minus 5°–10° for the last 10 Myr), which is comparable to the ~15°–20° clockwise rotations inferred for the Esk Head Melange prior to 10 Ma. Approximately constant rates of rotation across the entire margin during the early mid-Miocene are consistent with deformation across the Taranaki Fault (near to the western margin of the plate boundary zone) that occurred at this time but which has been largely absent in the last 5–10 Ma [*King and Thrasher*, 1996; *Nicol et al.*, 2004].

5. Margin-Parallel Motion

[33] The current rates of ca. 25–30 mm/year of total margin-parallel relative plate motion between latitudes 39° and 41.5°S [*Beavan et al.*, 2002] could produce 600–900 km of strike-slip if these rates applied since 24–30 Ma. However, even the long (for example, >100 km) strike-slip faults in the North Island Fault System collectively appear to carry no more than 20 km total strike-slip [*Beanland*, 1995; this study]. The apparent discrepancy between the estimated strike-slip and the total margin-parallel motion across the

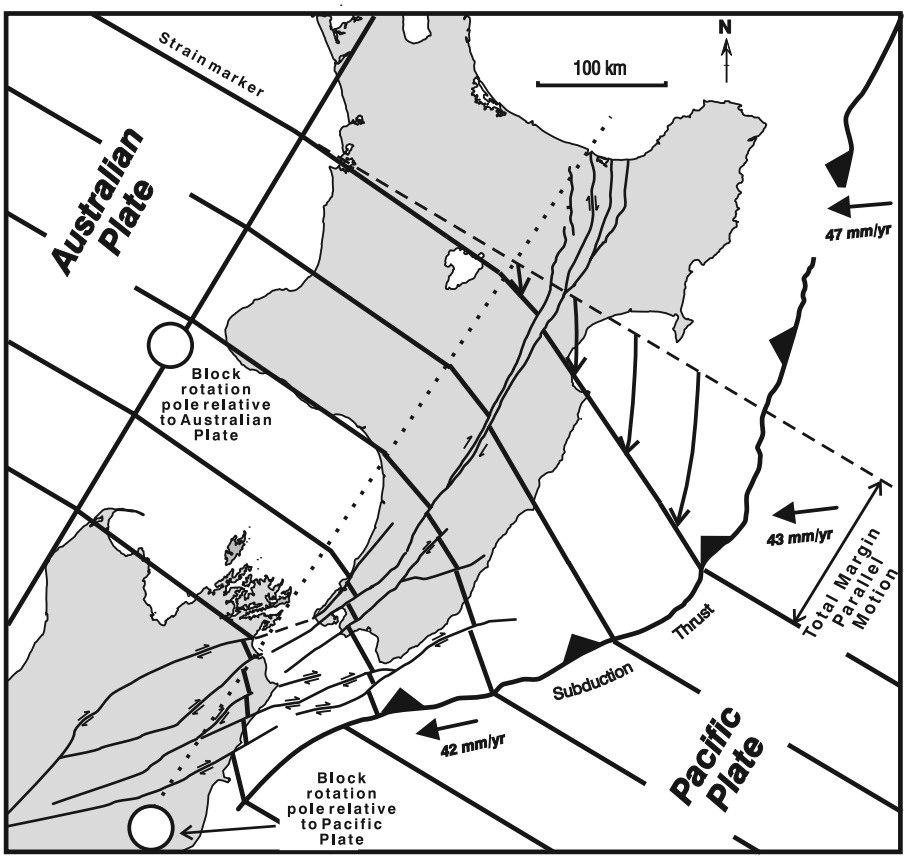

Figure 12. Schematic diagram of North Island showing strike-slip faults and clockwise rotations for marker lines oriented NW-SE at 10 Ma. Finite rotations of strain markers increase from west to east. The total margin-parallel motion due to strike-slip and vertical-axis rotations is shown. Bending of the Australian Plate takes place about an axis approximately coincident with the southern termination of subduction and the block rotation pole relative to a fixed Pacific Plate. The block rotation poles are from the work of *Wallace et al.* [2004]. For further discussion, see text.

margin require that either (1) significant strike-slip in the upper plate remains undetected, (2) strike-slip occurs on the plate interface, (3) the rates of margin-parallel motion were lower in the past than they are today, or (4) margin-parallel slip is being accommodated in the upper plate by clockwise vertical-axis rotation of the eastern North Island [e.g., *Wallace et al.*, 2004]. To explore which of these alternatives is most likely we estimate the margin-parallel motion due to the clockwise rotations of the Australian Plate and the total margin-parallel relative plate motion. The difference between these two measures indicates the maximum permissible strike-slip on upper plate faults.

[34] The rate of margin-parallel motion is controlled by the azimuth and magnitude of the relative plate motion vector and by the trend of the plate boundary. The motion of the Pacific Plate relative to the Australian Plate since 26 Ma is defined by rotations about a series of Euler poles located south of New Zealand [e.g., *Cande and Stock*, 2004]. The Australian/Pacific Plate relative motion vector is calculated here for a fixed location approximately midway along the Hikurangi Margin (i.e., latitude 40°S and longitude 179°E) using the location and rate of rotations about Euler poles from seafloor spreading information for 2.58–26.55 Ma [*Cande and Stock*, 2004, Table 7] and from contemporary GPS [*Beavan et al.*, 2002, Table 3]. Neither our choice of published Euler pole locations and rotation rates nor the location used for generating Figure 13 impact on the first-order conclusions presented here. The relative plate motion azimuth varied by 2° since ca. 26 Ma, while the southward migration of the Euler poles resulted in an increase of the rate of motion from 32 mm/year at ca. 26 Ma to 43 mm/year today [*Beavan et al.*, 2002; *Cande and Stock*, 2004]. In addition to these rate changes, the overriding plate rotated clockwise by ca. 45°–50° since 24–30 Ma. We follow previous literature in suggesting that rotations of the upper plate describe the rotation of the margin [e.g., *Walcott*, 1984a, 1987; *Rait et al.*, 1991; *Field et al.*, 1997; *King*, 2000]. Therefore, to chart the change in trend of the margin, we have used clockwise rotation rates of 2°–4°/Myr since 10 Ma and 0°–1°/Myr from ca. 10 to 26–30 Ma, as can be inferred from the paleomagnetic data. For these rates of rotation, a present margin trend of 030° and the Euler poles of *Cande and Stock* [2004] and *Beavan et al.* [2002], we estimate the margin-parallel and margin-normal components

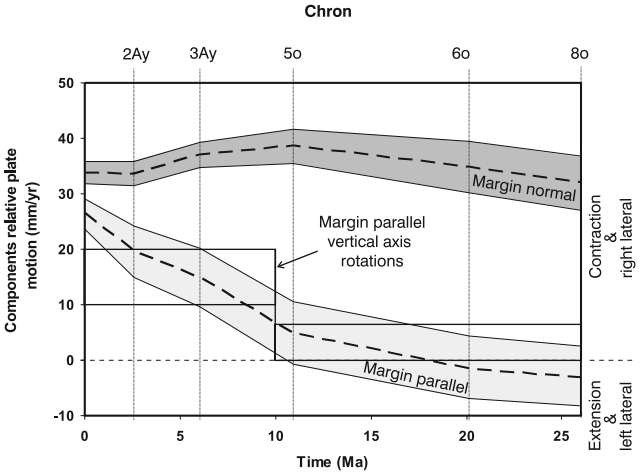

Figure 13. Margin-parallel and margin-normal components of the Pacific and Australian relative plate motion vector since ca. 26 Myr for the central Hikurangi Margin (latitude 40°S and longitude 179°E). Components of motion calculated using finite rotation poles for the Australian/Pacific plate boundary from 2.58- to 26.55-Ma seafloor spreading information of *Cande and Stock* [2004] and contemporary GPS of *Beavan et al.* [2002]. Margin orientations and the component of margin-parallel motion due to vertical-axis rotation calculated using a present margin trend of 030° and clockwise rotations of 3 ± 1°/Myr from 0–10 Ma and 0–1°/Myr from 10–26 Ma (see section 4). For relative plate motion components, dashed lines represent means, while shaded areas indicate standard errors. Paired horizontal lines indicate maximum and minimum margin-parallel motion accommodated by vertical-axis rotations.

of Australian/Pacific Plate relative motion vector at 0, 2.58, 6.04, 10.95, 20.13, and 26.55 Ma. As the plate motion azimuth remained approximately stable over the last 26 Myr, temporal changes in the margin-normal and margin-parallel components of relative plate motion (Figure 13) were due mainly to margin rotation and southward migration of the Euler pole.

[35] Clockwise rotation of the margin resulted in a progressive increase in the component of margin-parallel motion as subduction evolved (Figure 13). Prior to about 15 Ma the relative plate motion vector was approximately orthogonal to the margin, with little or no strike-slip required. A similar conclusion has been reached for margin rotations ca. 20°–40° greater than those used here and for comparable Euler pole locations [*Beanland*, 1995; *King*, 2000]. The rates of margin-parallel motion increased from about 10 Ma to the present, with current rates at a maximum for the post-Oligocene. Clockwise rotations could account for the entire margin-parallel component of the relative plate motion (see Figure 12 for derivation) prior to ca. 1–2 Ma (Figure 13), however, given the uncertainties in the total margin-parallel motion, in the margin-parallel accommodated by rotations and in the timing of the inferred change in rotation rates, some strike-slip before 1–2 Ma cannot be discounted. After ca. 1–2 Ma, rotations take up between ca. 35 and 85% of the total margin-parallel motion, with ca. 3–19 mm/year accommodated by other mechanisms (at the latitude of Figure 13). These numbers are consistent with the modeling of GPS velocities which suggest that ~60% of contemporary margin-parallel motion is accommodated by the clockwise rotation of the eastern North Island. Earthquake slip vectors from the subduction thrust [*Webb and Anderson*, 1998] and GPS [*Wallace et al.*, 2004] indicate that the contemporary slip on the subduction interface is mainly dip-slip. Therefore we infer that the nonrotational component of the margin-parallel motion was mainly accommodated by strike-slip faults in the upper plate. At the latitude of Figure 13, strike-slip in the North Island Fault System accounts for 30–100% of the nonrotational margin-parallel motion in the last 1–2 Myr (i.e., 6–12 mm/year; *Beanland* [1995]; *Schermer et al.* [2004]; *Langridge et al.* [2005]).

[36] Late Quaternary rates of strike-slip of ca. 6–8 mm/year on the Wellington Fault [*Berryman*, 1990] could have produced cumulative displacement of 5–8 km in the last 0.6–1.3 Ma, with little strike-slip prior to this time [see also *Berryman et al.*, 2002]. These calculations are consistent with the inferred 1- to 2-Ma age of strike-slip in the North Island Fault System [*Erdman and Kelsey*, 1992; *Beanland*, 1995; *Kelsey et al.*, 1995] and with the suggestion that, prior to 1–2 Ma, margin-parallel plate motion was mainly accommodated by vertical-axis rotations. These rotations also caused the margin to become more oblique to the relative plate motion vector through time, increasing the strike-slip required. With continued clockwise rotation of the margin we expect the role of strike-slip to increase in the future.

[37] For the Pacific-Australian relative plate motion the total margin-parallel right-lateral displacement since 26 Ma would have been ca. 190 ± 130 km, with ca. 150 ± 50 km in the last 10 Myr (Figure 13). Clockwise rotation over the same time periods (i.e., 0–26 and 0–10 Ma) produced about 200 ± 100 and 150 ± 50 km of margin-parallel motion. These estimates are consistent with the notion that the total margin-parallel motion was >100 km, with a significant proportion (for example, 50–100%) of this accommodated by clockwise rotation. Given the uncertainties, the precise relations between total and rotational margin-parallel motion are not known. Models requiring hundreds of kilometers of right-lateral strike-slip in the upper plate during the early Miocene [e.g., *Delteil et al.*, 1996] are, however, inconsistent with the available data, unless anticlockwise rotation or hundreds of kilometers of left-lateral strike-slip are introduced to reconcile upper plate right-lateral strike-slip and clockwise rotation with the relative plate motion.

6. Discussion

[38] At plate boundaries the spatial pattern of tectonic and depositional environments may change significantly through time. Under these circumstances, reconstructions of paleo-environments or paleogeography can be problematic if postreconstruction deformation has not been removed. This point has been widely recognized, and numerous

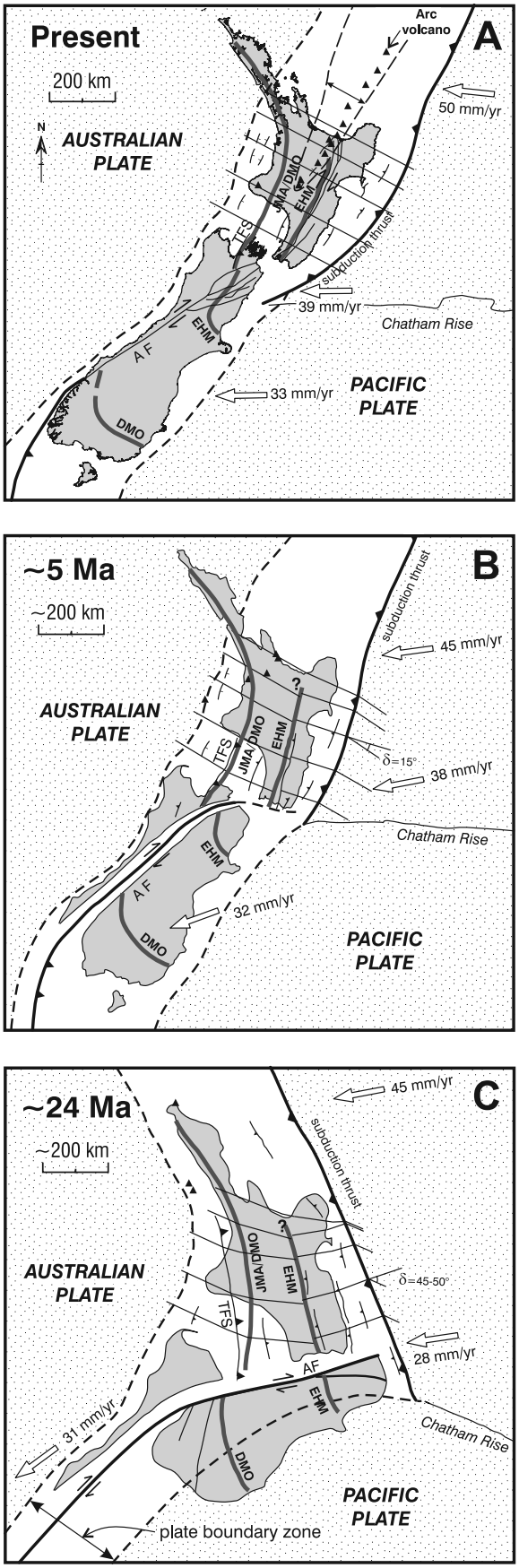

workers have produced Tertiary restorations of parts of [*Beu*, 1995; *Crampton et al.*, 2003] or the entire New Zealand plate boundary [e.g., *Ballance*, 1976; *Carter and Norris*, 1976; *Cole*, 1986; *Walcott*, 1978, 1987; *Kamp*, 1987; *Lamb*, 1988; *Rait et al.*, 1991; *Lewis and Pettinga*, 1993; *Field et al.*, 1997; *King*, 2000]. To test the validity of past reconstructions for the Hikurangi Margin, we use the strain profiles from Figures 3 and 4 in addition to paleomagnetic rotations, fault strike-slip, and bending of basement terranes. Tectonic restorations are presented for ca. 5 and 24 Ma using the present coastline and the transect lines from Figure 5 as reference lines to track deformation (Figure 14). Mean values of shortening, extension, strike-slip, and vertical axis rotations are used in all cases. The reconstructions should be regarded as first approximations with the older of the two considered less precise.

[39] The 5-Ma map does not show a significant change in shape of the coastline from the present configuration (for example, compare Figures 14a and 14b), while the 24-Ma tectonic reconstruction displays a change in shape of the coastline along with a change in the location and trend of the margin (Figures 14b and 14c). Neither map depicts as much deformation as previous reconstructions for the same two time lines [e.g., *Ballance*, 1976; *Carter and Norris*, 1976; *Walcott*, 1984a, 1984b, 1987; *Kamp*, 1987; *Rait et al.*, 1991; *King*, 2000]. The principal reasons for this departure from previous work are fourfold. First, in our reconstructions, the total extension across the Taupo Volcanic Zone and the Central Volcanic Region (see Figure 7) is significantly less than their total width (i.e., 2- to 38-km extension on strain profiles 23, 24, and 25 as opposed to 50–100 km width at the location of these profiles, Figure 7). This conclusion is consistent with the predominance of extension of continental crust and the absence of newly created oceanic crust in the onshore volcanic regions. Second, our

Figure 14. Reconstructions of New Zealand Plate boundary zone and the Hikurangi Margin from the (a) present to (b) 5 and (c) ~24 Ma. The locations of the strain transects in Figure 5 have been included as additional markers. The 5-Ma reconstruction includes up to 20 km (profile D) of shortening and 42 km (profile A) of extension, 5 km of distributed strike-slip across the entire margin and an additional 15 km of strike-slip on the North Island Fault System, 15° clockwise rotation of the eastern North Island (i.e., average rate 3°/Myr) and zero rotation at the western margin of the plate boundary. In addition to deformation over the last 5 Myr, the 24-Ma reconstruction includes 30° clockwise rotation (see section 4), no strike-slip, and 115 km of margin-normal shortening distributed across the entire plate boundary zone at a latitude of 40°S (for example, sum profiles 41, 49, and 63). TFS is the Taranaki Fault System (includes the Taranaki, Manaia, and Waimea-Flaxmore faults); AF, Alpine Fault; DMO, Dun Mountain Ophiolite; EHM, Esk Head Melange. Open arrows and rates indicate motion of the Pacific Plate relative to the Australian Plate for the present-day [*Beavan et al.*, 2002] and the geological record [*Cande and Stock*, 2004].

results indicate that margin-parallel plate motion was mostly accommodated by clockwise rotations about vertical axes, significantly decreasing the requirement for strike-slip faulting. Third, the total post-Oligocene clockwise rotation of 45°–50° for the eastern 100–200 km of the margin is significantly less than the 60°–90° typically applied for this region. Increasing the rotations by a factor of two would be expected to increase the margin-normal shortening across the entire plate boundary zone in the southern North Island by a similar order. While substantial (>20–30 km) early Miocene shortening and thrusting has been inferred along the east coast of the North Island [e.g., *Pettinga*, 1982; *Rait et al.*, 1991; *Barnes et al.*, 2002] and Raukumara Peninsula [*Mazengarb and Speden*, 2000], the available data does not support Miocene shortening in excess of about 150 km (Figure 10c). Last, the ca. 3–8 mm/year average rates of margin-normal shortening in the upper plate were much lower than the average 34–35 mm/year rate of plate convergence since the Oligocene (Figure 13). Therefore most (>80% at latitude 40°30′S) of the convergence across the plate boundary accrued on the plate interface, making the subduction thrust by far the most important contractional structure along the Hikurangi Margin since the inferred inception of subduction [*Nicol and Beavan*, 2003; *Nicol and Wallace*, 2007; this study]. Shortening rates in the upper plate for the Miocene and post-Miocene time intervals are consistent with the view that, when averaged for ≥5 Myr, both the plate convergence rates and the transfer of displacement from the subduction thrust into the upper plate was approximately constant.

[40] Uniform rates of shortening in the upper plate were accompanied by variable strike-slip, normal faulting, and clockwise rotations. The increase in strike-slip is, at least in part, driven by the temporal and spatial increase in the obliquity of relative plate motion, with lower rates of margin-parallel plate motion during the Miocene than the Pliocene-Pleistocene. In addition, the southward increase of strike-slip along the margin during the last 1–2 Myr may also be influenced by a narrowing of the width of the plate boundary and a consequent reduction in the margin-parallel motion accommodated by clockwise rotations [*Nicol and Wallace*, 2007]. Normal faulting in the northwestern North Island, including rifting in the Taupo Volcanic Zone, formed in conjunction with rotations of the eastern Hikurangi Margin [*Wallace et al.*, 2004]. These clockwise rotations are thought to arise, in part, because the subduction thrust has no finite slip at its southern termination, where continental collision is taking place, and is slipping freely beneath Raukumara Peninsula [*Reyners*, 1998; *Upton et al.*, 2003; *Wallace et al.*, 2004]. The 5- and 24-Ma reconstructions also incorporate slab rollback, which has been proposed to account for the eastward migration and apparent clockwise swing in the trend of volcanic arcs from 40 Ma to the present [e.g., *Ballance*, 1976; *Walcott*, 1987; *Stratford and Stern*, 2006]. Increases in the rates of rotation at about 10 Ma may signify an increase in the rate (or the commencement) of slab rollback at this time and/or could signify the onset of subduction of the Hikurangi Plateau. An increase in rotation rates at about 10 Ma would be consistent with an increase in the rate of extension in the Taranaki Basin at this time.

[41] Figures 13 and 14 allow us to speculate as to why the search for major strike-slip faults in the North Island (for example, >50- to 100-km displacement) has been unsuccessful. During the early to middle Miocene (ca. 10–24 Ma) the Hikurangi Margin was approximately orthogonal to the Alpine Fault and the relative plate motion vector (Figures 13 and 14c). Given these fault geometries and kinematics, there is no requirement for strike-slip in the Hikurangi Margin, and strike-slip on the Alpine Fault would have been transferred onto the subduction thrust as dip-slip or into the overriding plate as shortening (Figure 14). Clockwise rotation of the Hikurangi Margin contributed to a progressive decrease in the angle between the trend of the margin and the strike of the Alpine Fault since 24 Ma (compare Figures 14b and 14c). As a result, more Alpine Fault strike-slip was transferred into strike-slip and vertical-axis rotations in the Hikurangi Margin as subduction progressed. Strike-slip in the upper plate appears to have commenced late in the evolution of the margin at 1–2 Ma [*Erdman and Kelsey*, 1992; *Kelsey et al.*, 1995; this study], with high rates of strike-slip (>10 mm/year) mainly limited to the southernmost 100 km of the North Island Fault System. The North Island Fault System is presently the most likely northern extension of the Alpine Fault in the North Island. However, because of the North Island Fault Systems comparatively short strike-slip history and because much of the Alpine Fault displacement is (and has been in the past) transferred directly onto the subduction thrust, it only carries a small fraction of the total displacement on the Alpine Fault in the northern South Island.

7. Conclusions

[42] Deformation of the Hikurangi Margin, New Zealand has been driven by the subduction of the Pacific Plate during the last 24–30 Ma and includes shortening, extension, vertical-axis rotations, and strike-slip faulting. Shortening in the upper plate increased southward reaching a maximum of ca. 3–8 mm/year. Shortening in the upper plate since the Oligocene accommodated a small proportion of the rate of plate convergence, with most (>80%) accruing on the subduction thrust. The uniformity of these rates of upper plate shortening are consistent with the near-constant rates of plate convergence and suggest that, when averaged for ≥5 Myr, the transfer of displacement from the subduction thrust into the upper plate was also approximately uniform. In contrast to the temporal uniformity of the shortening, the rates of clockwise vertical-axis rotations of the eastern Hikurangi Margin were variable, with higher rates since 10 Ma (∼3°/Myr) than between 10 and 30 Ma (∼0°–1°/Myr). During the last 10 Myr the rates of rotation decreased with increasing distance westward from the subduction thrust, which resulted in bending of the North Island about an axis coincident with the southern termination of subduction. With the rotation of the margin and southward migration of the Pacific Plate Euler poles, the component of margin-parallel relative plate motion has increased to the present. Plate convergence dominated the Hikurangi Margin

before ca. 15 Ma, with the rate of margin-parallel motion increasing markedly since 10 Ma. Vertical-axis rotations could have accounted for all of the margin-parallel motion before 1–2 Ma and the onset of strike-slip in the North Island Fault System, eliminating the necessity for large strike-slip displacements (for example, >50 km) in the overriding plate.

[43] **Acknowledgments.** Funding for this work was provided by the New Zealand Foundation for Research, Science and Technology. Discussions with Kelvin Berryman, Susan Ellis, and Peter King were of great benefit. Phil Barnes, Peter King, Vaughan Stagpoole, Dougal Townsend, Richard Norris, Harvey Kelsey, and an anonymous reviewer provided constructive comments on early versions of this manuscript.

References

Anderton, P. W. (1981), Structure and evolution of the south Wanganui Basin, New Zealand, *N. Z. J. Geol. Geophys.*, *24*, 39–63.

Bannister, S. C. (1988), Microseismicity and velocity structure in the Hawkes Bay region, New Zealand: Fine structure of the subducting Pacific plate, *Geophys. J. R. Astron. Soc.*, *95*, 45–62.

Ballance, P. F. (1976), Evolution of the upper Cenozoic magmatic arc and plate boundary in northern New Zealand, *Earth Planet. Sci. Lett.*, *28*, 356–370.

Barnes, P. M., and J. C. Audru (1999), Quaternary faulting in the offshore Flaxbourne and Wairarapa basins, southern Cook Strait, New Zealand, *N. Z. J. Geol. Geophys.*, *42*, 349–367.

Barnes, P. M., and A. Nicol (2004), Formation of an active thrust triangle zone associated with structural inversion in a subduction setting, eastern New Zealand, *Tectonics*, *23*, TC1015, doi:10.1029/2002TC001449.

Barnes, P. M., and B. M. Mercier de Lépinay (1997), Rates and mechanics of rapid frontal accretion along the very obliquely convergent southern Hikurangi Margin, New Zealand, *J. Geophys. Res.*, *102*, 24,931–24,952.

Barnes, P. M., B. Mercier de Lepinay, J.-Y. Collot, J. Delteil, and J.-C. Audru (1998), Strain partitioning in the transition area between oblique subduction and continental collision, Hikurangi Margin, New Zealand, *Tectonics*, *17*(4), 534–557.

Barnes, P. M., A. Nicol, and A. Harrison (2002), Late Cenozoic evolution and earthquake potential of an active listric thrust complex, Hikurangi subduction margin, New Zealand, *Geol. Soc. Am. Bull.*, *114*, 1379–1405.

Barnett, J. A. M., J. Mortimer, J. H. Rippon, J. J. Walsh, and J. Watterson (1987), Displacement geometry in the volume containing a single normal fault, *Am. Assoc. Pet. Geol. Bull.*, *71*, 925–937.

Beanland, S. (1995), The North Island dextral fault belt, Hikurangi subduction margin, New Zealand, Ph.D. thesis, Victoria Univ. of Wellington, Wellington, New Zealand.

Beanland, S., and K. Berryman (1987), Ruahine fault reconnaissance, N. Z. Geol. Surv. EDS reports 109.

Beanland, S., and A. J. Haines (1998), A kinematic model of active deformation in the North Island, New Zealand, determined from geological strain rates, *N. Z. J. Geol. Geophys.*, *41*, 311–323.

Beanland, S., A. Melhuish, A. Nicol, and J. Ravens (1998), Structure and deformation history of the inner forearc region, Hikurangi subduction margin, New Zealand, *N. Z. J. Geol. Geophys.*, *41*, 325–342.

Beavan, J., and J. Haines (2001), Contemporary horizontal velocity and strain-rate fields of the Pacific-Australian plate boundary zone through New Zealand, *J. Geophys. Res.*, *106*, 741–770.

Beavan, J., P. Tregoning, B. Bevis, T. Kato, and C. Meertens (2002), The motion and rigidity of the Pacific Plate and implications for plate boundary deformation, *J. Geophys. Res.*, *107*(B10), 2261, doi:10.1029/2001JB000282.

Begg, J. G., and M. R. Johnston (compilers) (2002), Geology of the Wellington area, Inst. Geol. Nucl. Sci. geological map 10, scale 1:250,000, 1 sheet + 64 p.

Begg, J. G., and C. Mazengarb (1996), Geology of the Wellington area, Sheet R27, R28, part Q27, Inst. Geol. Nucl. Sci. map 22, scale 1:50,000, 3 sheets.

Benson, W. N. (1952), Meeting of the Geological Division of the Pacific Science congress in New Zealand, February, 1949, Int. Proc. Geol. Soc. Am., 1950, 11–13.

Berryman, K. R. (1990), Late Quaternary movement on the Wellington Fault in the Upper Hutt area, New Zealand, *N. Z. J. Geol. Geophys.*, *33*, 257–270.

Berryman, K., and S. Beanland (1988), Ongoing deformation in New Zealand: Rates of tectonic movement from geological evidence, *Trans. Inst. Prof. Eng. N. Z.*, *15*, 25–35.

Berryman, K., and S. Beanland (1991), Variation in fault behaviour in different tectonic provinces of New Zealand, *J. Struct. Geol.*, *13*, 177–189.

Berryman, K., R. Van Dissen, and V. Mouslopoulou (2002), Recent rupture of the Tararua section of the Wellington Fault and relationships to other faults section and rupture segments, Inst. Geol. Nucl. Sci. EQC research report, 97/248.

Beu, A. G. (1995), Pliocene limestones and their scallops, *Inst. Geol. Nucl. Sci. Monogr.*, *10*, 243 p.

Cande, S. C., and J. Stock (2004), Pacific-Antarctic-Australian motion and the formation of the Macquarie Plate, *Geophys. J. Int.*, *157*, 399–414.

Cape, C. D., S. H. Lamb, P. Vella, P. E. Wells, and D. J. Woodward (1990), Geological structure of Wairarapa Valley, New Zealand, from seismic reflection profiling, *J. R. Soc. N. Z.*, *20*, 85–105.

Carter, R. M., and R. J. Norris (1976), Cainozoic history of southern New Zealand: An accord between geological observation and plate tectonic predictions, *Earth Planet. Sci. Lett.*, *31*, 85–94.

Cashman, S. M., and H. M. Kelsey (1990), Forearc uplift and extension, southern Hawke's Bay, New Zealand, mid-Pleistocene to present, *Tectonics*, *9*, 23–44.

Cashman, S. M., H. M. Kelsey, C. F. Erdman, H. N. C. Cutten, and K. R. Berryman (1992), Strain partitioning between structural domains in the forearc of the Hikurangi subduction zone, New Zealand, *Tectonics*, *11*, 242–257.

Chanier, F. (1991), Le Prisme d'accrétion Hikurangi: un témoin de l'évolution géodynamique d'une marge active péripacifique (Nouvelle-Zélande) [Thèse de Doctorat]: Flandres-Artois, de l'Université des Sciences et Techniques de Lille, France.

Chanier, F., and J. Ferriere (1989), Sur L'existence de mouvements tangentiels majeurs dans la chaine côtiere orientale de Nouvelle-Zélande; signification dans le cadre de la subduction de la Plaque Pacifique, *Comptes Rendus de l'Academie des Sciences, Paris*, *308*, 1645–1650.

Chanier, F., and J. Ferriere (1991), From a passive to an active margin: tectonic and sedimentary processes linked to the birth of an accretionary prism (Hikurangi Margin, New Zealand), *Bulletin Societe Geologique de la France*, *162*, 469–660.

Chanier, F., J. Ferriere, and J. Angelier (1999), Extensional deformation across an active margin, relations with subsidence, uplift, and rotations: The Hikurangi subduction, New Zealand, *Tectonics*, *18*(5), 862–876.

Chapman, G. R., S. J. Lippard, and J. E. Martyn (1978), The stratigraphy and structure of the Kamasia Range, Kenya Rift Valley, *J. Geol. Soc. Lond.*, *135*, 265–281.

Cole, J. W. (1986), Distribution and tectonic setting of late Cenozoic volcanism in New Zealand, in *Late Cenozoic Volcanism in New Zealand*, edited by I. E. M. Smith, *R. Soc. N. Z. Bull.*, *23*, 7–20.

Cole, J. W., D. J. Darby, and T. A. Stern (1995), Taupo Volcanic Zone and Central Volcanic Region—Back arc structures of North Island, New Zealand, in Back-arc basins: Tectonism and magmatism, edited by B. Taylor, 1–28, Springer, New York.

Collot, J. V., et al. (1996), From oblique subduction to intra-continental transpression: Structures of the Southern Kermadic-Hikurangi Margin from multibeam bathymetry, side-scan conar and seismic reflection, *Mar. Geophys. Res.*, *18*, 357–381.

Cooper, R. A. (Ed) (2004), The New Zealand Geological Timescale., *Ins. Geol. Nucl. Sci. Monogr.*, *22*, 284 pp.

Crampton, J., M. Laird, A. Nicol, D. Townsend, and R. Van Dissen (2003), Palinspastic reconstructions of Southeastern Marlborough, New Zealand, for mid-Cretaceous-Eocene times, *N. Z. J. Geol. Geophys.*, *46*, 153–175.

Davey, F. J., M. Hampton, J. R. Childs, M. A. Fisher, K. B. Lewis, and J. R. Pettinga (1986a), Structure of a growing accretionary prism, Hikurangi Margin, New Zealand, *Geology*, *14*, 663–666.

Davey, F. J., K. B. Lewis, J. R. Childs, and M. Hampton (1986b), Convergent margin off east coast of North Island, New Zealand, Parts I and II, in *Seismic Images of Modern Convergent Margin Tectonic Structure*, edited by R. E. Von Huene, *Am. Assoc. Pet. Geol. Stud. Geol.*, *26*, 49–53.

Davey, F. J., S. A. Henrys, and E. Lodolo (1995), Asymmetric rifting in a continental back-arc environment, North Island, New Zealand, *J. Volcanol. Geotherm. Res.*, *68*, 209–238.

Delteil, J., H. E. G. Morgans, J. I. Raine, B. D. Field, and H. N. C. Cutten (1996), Early Miocene thin-skinned tectonics and wrench faulting in the Pongaroa district, Hikurangi Margin, North Island, New Zealand, *N. Z. J. Geol. Geophys.*, *39*, 271–282.

DeMets, C., R. G. Gordon, D. F. Argus, and S. Stein (1994), Effect of recent revisions to the geomagnetic reversal time scale on estimates of current plate motions, *Geophys. Res. Lett.*, *21*, 2191–2194.

Edbrooke, S. W. (compiler) (2001), Geology of the Auckland area: Institute of Geological and Nuclear Sciences geological map 3, scale 1:250,000, 1 sheet + 74 p.

Erdman, C. F., and H. M. Kelsey (1992), Pliocene and Pleistocene stratigraphy and tectonics, Ohara Depression and Wakarara Range, North Island, New Zealand, *N. Z. J. Geol. Geophys.*, *35*, 177–192.

Field, B. D., C. I. Uruski, et al. (1997), Cretaceous-Cenozoic geology and petroleum systems of the East Coast Region, New Zealand. Institute of Geological and Nuclear Sciences monograph, *19*: 301, 7 enclosures, Inst. Geol. Nucl. Sci. Ltd., Lower Hutt, New Zealand.

Grapes, R. H. (1991), Aggradation surfaces and implications for displacement rates along the Wairarapa Fault, southern North Island, New Zealand, *Catena*, *18*, 453–469.

Grapes, R. H., and H. W. Wellman (1988), The Wairarapa Fault, Res. School of Earth Science, Geology

Board of Stud, Victoria Univ. of Wellington, Wellington, New Zealand, pub. 4, 55 pp.

Gutscher, M.-A., N. Kukowski, J. Malavieille, and S. Lallemand (1998), Material transfer in accretionary wedges from analysis of a systematic series of analog experiments, *J. Struct. Geol.*, *20*, 407–416.

Henrys, S., M. Reyners, I. Pecher, S. Bannister, Y. Nishimura, and G. Maslen (2006), Kinking of the subducting slab by escalator normal faulting beneath the North Island of New Zealand, *Geology*, *34*, 777–780, doi:10.1130/G22594.1.

Holt, W. E., and T. A. Stern (1994), Subduction, platform subsidence, and foreland thrust loading: The late Tertiary development of Taranaki Basin, New Zealand, *Tectonics*, *13*, 1068–1092.

Idnurm, M. (1985), Late Mesozoic and Cenozoic palaeomagnetism of Australia: 1. A redetermined apparent polar wander path, *Geophys. J. R. Astron. Soc.*, *83*, 399–418.

Kamp, P. J. J. (1987), Age and origin of the New Zealand Orocline in relation to Alpine Fault movement, *J. Geol. Soc. Lond.*, *144*, 641–652.

Kamp, P. J. J. (1999), Tracking crustal processes by FT thermochronology in a forearc high (Hikurangi margin, New Zealand) involving Cretaceous subduction termination and mid-Cenozoic subduction initiation, *Tectonophysics*, *307*, 313–343.

Kelsey, H. M., C. F. Erdman, and S. M. Cashman (1993), Geology of southern Hawkes Bay from the Maraetotara plateau and Waipawa westward to the Wakarara Range and the Ohara Depression, Inst. Geol. Nucl. Sci. science report 93/2, 17 pp.

Kelsey, H. M., S. M. Cashman, S. Beanland, and K. R. Berryman (1995), Structural evolution along the inner forearc of the obliquely convergent Hikurangi Margin, New Zealand, *Tectonics*, *14*, 1–18.

Kelsey, H. M., A. G. Hull, S. M. Cashman, K. R. Berryman, P. H. Cashman, J. H. Trexler, and J. G. Begg (1998), Paleoseismology of an active reverse fault in a forearc setting: The Poukawa Fault Zone, Hikurangi Margin, New Zealand, *Geol. Soc. Am. Bull.*, *110*, 1123–1148.

Kennett, J. P., and N. D. Watkins (1974), Late Miocene - Early Pliocene paleomagnetic stratigraphy, paleoclimatology, and biostratigraphy in New Zealand, *Geol. Soc. Am. Bull.*, *85*, 1385–1398.

King, P. B. (2000), Tectonic reconstructions of New Zealand: 40 Ma to the Present, *N. Z. J. Geol. Geophys.*, *43*, 611–638.

King, P. R., and G. P. Thrasher (1996), Cretaceous-Cenozoic geology and petroleum systems of the Taranaki Basin, New Zealand, *Inst. Geol. Nucl. Sci.*, 13.

Kingma, J. T. (1958), Possible origin of piercement structures, local unconformities, and secondary basins in the eastern geosyncline, New Zealand, *N. Z. J. Geol. Geophys.*, *12*, 269–274.

Lamarche, G., S. Beanland, and J. Ravens (1995), Deformation style and history of the Eketahuna region, Hikurangi forearc, New Zealand, from shallow seismic reflection data, *N. Z. J. Geol. Geophys.*, *38*, 105–115.

Lamarche, G., J. M. Bull, P. M. Barnes, S. K. Taylor, and H. Horgan (2000), Constraining fault growth rates and fault evolution in New Zealand, *Eos Trans. AGU*, *81*, 481, 485, 486.

Lamb, S. H. (1988), Tectonic rotations about vertical axes during the last 4 Ma in part of the New Zealand plate-boundary zone, *J. Struct. Geol.*, *10*, 874–893.

Langridge, R. M., K. R. Berryman, and R. J. Van Dissen (2005), Defining the geometric segmentation and Holocene slip rate of the Wellington Fault, New Zealand: The Pahiatua section, *N. Z. J. Geol. Geophys.*, *48*, 591–607.

Lee, J. M., and J. G. Begg (2002), Geology of the Wairarapa area. Institute of Geological and Nuclear Sciences 1:250 000 geological map 11. 1 sheet + 66 p, Inst. Geol. Nucl. Sci. Ltd., Lower Hutt, New Zealand.

Lewis, K., and J. R. Pettinga (1993), The emerging, imbricate frontal wedge of the Hikurangi margin, in South Pacific sedimentary basins, Sedimentary Basins of the World, *2*, edited by P. F. Ballance, 225–250, series editor, K. Hsu.

Little, T. A., and A. P. Roberts (1997), Distribution and mechanism of Neogene to present-day vertical axis rotations, Pacific-Australian Plate boundary zone, South Island, New Zealand, *J. Geophys. Res.*, *102*, 20,447–20,468.

Little, T. A., R. Grapes, and G. W. Berger (1998), Late Quaternary strike slip on the eastern part of the Awatere Fault, South Island, New Zealand, *Geol. Soc. Am. Bull.*, *110*, 127–148.

Mazengarb, C., and I. G. Speden (2000), Geology of Raukumara Penninsula. Institute of Geological and Nuclear Sciences 1:250 000 geological map 6. 1 sheet and p. 60.

Melhuish, A. (1990), Late Cenozoic deformation along the Pacific-Australian plate margin, Dannevirke region, New Zealand, M.Sc. thesis, Victoria Univ. of Wellington, New Zealand.

Mortimer, N. (1995), Origin of the Torlesse Terrane and coeval rocks, North Island, New Zealand, *Int. Geol. Rev.*, *36*, 891–910.

Mouslopoulou, V., A. Nicol, T. A. Little, and J. J. Walsh (2007), Terminations of large strike-slip faults: an alternative model from New Zealand, In: *Tectonics of Strike-Slip Restraining and Releasing Bends in Continental and Oceanic Settings*, Geol. Soc. London, Spec. Publ., in press.

Mumme, T. C., and R. I. Walcott (1985), Paleomagnetic studies at Geophysics Division 1980–1983.

Mumme, T. C., S. H. Lamb, and R. I. Walcott (1989), The Raukumara paleomagnetic domain: constraints on the tectonic rotation of the east coast, North Island, New Zealand, from paleomagnetic data, *N. Z. J. Geol. Geophys.*, *32*, 317–326.

New Zealand Geological Survey, North Island (1st Ed.) (1972), "Geological Map of New Zealand 1:1 000 000", Department of Scientific and Industrial Research, Wellington, New Zealand.

Nicol, A., and J. Beavan (2003), Shortening of an overriding plate and its implications for slip on a subduction thrust, central Hikurangi Margin, New Zealand, *Tectonics*, *22*(6), 1070, doi:10.1029/2003TC001521.

Nicol, A., and J. K. Campbell (1990), Late Cenozoic thrust tectonics, Picton, New Zealand, *N. Z. J. Geol. Geophys.*, *33*, 485–494.

Nicol, A., and C. Uruski (2005), Structural interpretation and cross section balancing, East Coast Basin, New Zealand, Institute of Geological and Nuclear Sciences Client Report 2005/117 9p plus 4 enclosures.

Nicol, A., and L. M. Wallace (2007), Temporal stability of deformation rates: Comparison of geological and geodetic observations, Hikurangi subduction margin, New Zealand, *Earth Planet Sci. Lett*, doi:10.1016/j.epsl.2007.03.039.

Nicol, A., R. Van Dissen, P. Vella, B. Alloway, and A. Melhuish (2002), Growth of contractional structures during the last 10 Ma, Hikurangi forearc, New Zealand, *N. Z. J. Geol. Geophys.*, *45*, 365–385.

Nicol, A., V. Stagpoole, and G. Maslen (2004), Structure and petroleum potential of the Taranaki Fault play. New Zealand Petroleum Conference Proceedings, Auckland 7–10 March 2004, http://www.crownminerals.govt.nz/petroleum/docs/nzpconf-2004/27-paper.pdf.

Pettinga, J. R. (1982), Upper Cenozoic structural history, coastal southern Hawkes Bay, New Zealand, *N. Z. J. Geol. Geophys.*, *25*, 149–191.

Pettinga, J. R., and D. U. Wise (1994), Paleostress adjacent to the Alpine fault: Broader implications from fault analysis near Nelson, South Island, New Zealand, *J. Geophys. Res.*, *99*, 2727–2736.

Rait, G. J. (1997), Large magnitude Miocene strike-slip on the North Island's East Coast?, *Geol. Soc. N. Z. Misc. Pub.*, *95a*, 140.

Rait, G. J. (2000), Thrust transport directions in the Northland Allochthon, New Zealand, *N. Z. J. Geol. Geophys.*, *43*, 271–288.

Rait, G., F. Chanier, and D. Waters (1991), Landward and seaward-directed thrusting accompanying the onset of subduction beneath New Zealand, *Geology*, *19, 230–233.*

Rattenbury, M. S., R. A. Cooper, and M. R. Johnston (1998), Geology of the Nelson area, Institute of Geological and nuclear Science 1:250,000 geological map 9 1 map (1 sheet) and booklet (67 p.), Inst. Geol. Nucl. Sci., Lower Hutt, New Zealand.

Raub, M. L. (1985), The neotectonic evolution of the Wakarara area, southern Hawkes Bay, New Zealand, M.Sc. thesis, Univ. of Auckland, Auckland, New Zealand.

Raub, M. L., H. N. C. Cutten, and A. G. Hull (1987), Seismotectonic hazard analysis of the Mohaka fault, North Island, New Zealand, Proceedings of Pacific conference on earthquake engineering, *Wellington, N. Z. Nat. Soc. Earthquake Eng.*, *3*, 219–230.

Reyners, M. (1998), Plate coupling and the hazard of large subduction thrust earthquakes at the Hikurangi subduction zone, New Zealand, *N. Z. J. Geol. Geophys.*, *41*, 343–354.

Reyners, M., and P. McGinty (1999), Shallow subduction tectonics in the Raukumara Peninsula, New Zealand, as illuminated by earthquake focal mechanics, *J. Geophys. Res.*, *104*, 3025–3034.

Reyners, M., D. Eberhart-Phillips, and G. Stuart (1999), A three-dimensional image of shallow subduction: crustal structure of the Raukumara Peninsula, New Zealand, *Geophys. J. Int.*, *137*, 873–890.

Reyners, M., D. Eberhart-Phillips, G. Stuart, and Y. Nishimura (2006), Imsubduction from the trench to 300 km depth beneath the central North Island, New Zealand, with Vp and Vp/Vs, *Geophys. J. Int.*, *165*, 565–583.

Roberts, A. P. (1992), Paleomagnetic constrints on the tectonic rotation of the southern Hikurangi Margin, New Zealand, *N. Z. J. Geol. Geophys.*, *35*, 311–323.

Roberts, A. P. (1995), Tectonic rotation about the termination of a major strike-slip fault, Marlborough Fault System, New Zealand, *Geophys. Res. Lett.*, *22*, 187–190.

Rowan, C. J., A. P. Roberts, and G. J. Rait (2005), Relocation of the tectonic boundary between the Raukumara and Wairoa Domains (East Coast, North Island, New Zealand): Implications for the rotation history of the Hikurangi Margin, *N. Z. J. Geol. Geophys.*, *48*, 185–196.

Schermer, E. R., R. Van Dissen, K. R. Berryman, H. M. Kelsey, and S. M. Cashman (2004), Active faults, paleoseismology, and historical fault rupture in the northern Wairarapa, North Island, New Zealand, *N. Z. J. Geol. Geophys.*, *47*, 101–122.

Stern, T. A., W. R. Stratford, and M. L. Salmon (2006), Subduction evolution and mantle dynamics at a continental margin: Central North Island, New Zealand, *Rev. Geophys.*, *44*, RG4002, doi:10.1029/2005RG000171.

Stock, J., and P. Molnar (1982), Uncertainties in the relative positions of the Australian, Antarctica, Lord Howe and Pacific plates since the Late Cretaceous, *J. Geophys. Res.*, *87*, 4679–4714.

Stratford, W. R., and T. A. Stern (2006), Crust and upper mantle structure of a continental backarc: Central North Island, New Zealand, *Geophys. J. Int.*, *166*, 469–484, doi:10.1111/j.1365-246X.2006.02967.x.

Sutherland, R. (1995), The Australia-Pacific boundary and Cenozoic plate motions in the SW Pacific: Some constraints from Geosat data, *Tectonics*, *14*, 819–831.

Thornley, S. (1996), Neogene tectonics of Raukumara Peninsula, northern Hikurangi margin, New Zealand, Ph.D. thesis. Victoria Univ. of Wellington, Wellington, New Zealand.

Thrasher, G. P., P. R. King, and R. A. Cook (1995), Taranaki Basin petroleum atlas. 50 maps plus booklet, Inst. Geol. Nucl. Sci. Ltd.

Tikoff, B., and K. Peterson (1998), Physical experiments of transpressional folding, *J. Struct. Geol.*, *20*, 661–672.

Upton, P., P. O. Koons, and D. Eberhart-Phillips (2003), Extension and partitioning in an oblique subduction zone, New Zealand: Constraints from three-dimensional numerical modelling, *Tectonics*, *22*(6), 1068, doi:10.1029/2002TC001431.

Uruski, C. I. (1998), Wanganui Basin seismic maps, Institute of Geological and Nuclear Sciences client report. 54767A.12, 16 p + maps.

Van Dissen, R. J., and K. R. Berryman (1996), Surface rupture earthquakes over the last ~1000 years in the Wellington region, New Zealand, and implications for ground shaking hazard, *J. Geophys. Res.*, *101*, 5999–6019.

Van Dissen, R. J., K. R. Berryman, J. R. Pettinga, and N. L. Hill (1992), Paleoseismicity of the Wellington-Hutt Valley segment of the Wellington Fault, North Island, New Zealand, *N. Z. J. Geol. Geophys.*, *35*, 165–176.

Villamor, P., and K. Berryman (2001), Quaternary extension rates derived from fault slip data in the Taupo Volcanic Zone, New Zealand, *N. Z. J. Geol. Geophys.*, *44*, 243–269.

Walcott, R. I. (1978), Present tectonics and late Cenozoic evolution of New Zealand, *Geophys. J. R. Astron. Soc.*, *52*, 137–164.

Walcott, R. I. (1984a), Reconstructions of the New Zealand region for the Neogene, *Palaeogeogr. Palaeoclimatol. Palaeoecol.*, *46*, 217–231.

Walcott, R. I. (1984b), The kinematics of the plate boundary zone through New Zealand: A comparison of short- and long-term deformations, *Geophys. J. R. Astron. Soc.*, *79*, 613–633.

Walcott, R. I. (1987), Geodetic strain and the deformational history of the North Island of New Zealand during the late Cainozoic, *Philos. Trans. R. Soc. London*, *A321*, 163–181.

Walcott, R. I. (1989), Paleomagnetically observed rotations along the Hikurangi margin of New Zealand, in Paleomagnetic rotations and continental deformation, edited by C. Kissel and C. Laj, Springer, New York, 459–471.

Walcott, R. I., D. A. Christoffel, and T. C. Mumme (1981), Bending within the axial tectonic belt of New Zealand in the last 9 Myr from paleomagnetic data, *Earth Planet. Sci. Lett.*, *52*, 427–434.

Wallace, L., J. Beavan, R. McCaffrey, and D. Darby (2004), Subduction zone coupling and tectonic block rotations in the North Island, New Zealand, *J. Geophys. Res.*, *109*(B12), B12406, doi:10.1029/2004JB003241.

Webb, T. H., and H. J. Anderson (1998), Focal mechanisms of large earthquakes in the North Island of New Zealand: Slip partitioning at an oblique active margin, *Geophys. J. Int.*, *134*, 40–86.

Wesnousky, S. G. (1988), Seismological and structural evolution of strike-slip faults, *Nature*, *335*, 340–343.

Wilson, G. S., and D. M. McGuire (1995), Distributed deformation due to coupling across a subduction thrust; mechanism of young tectonic rotation within the south Wanganui Basin, New Zealand, *Geology*, *23*, 645–648.

Wilson, C. J. N., B. F. Houghton, M. O. McWilliams, M. A. Lanphere, S. D. Weaver, and R. M. Briggs (1995), Volcanic and structural evolution of the Taupo Volcanic Zone, New Zealand: A review, *J. Volcanol. Geotherm. Res.*, *68*, 1–28.

Wright, I. C., and R. I. Walcott (1986), Large tectonic rotation of part of New Zealand in the last 5 Ma, *Earth Planet. Sci. Lett.*, *80*, 348–352.

F. Chanier, UMR CNRS - 8110, Processus et Bilans des Domaines Sédimentaires, Université des Sciences et Technologies de Lille 1, Bat. S.N.5, 59655, Villeneuve d'Ascq Cedex, France.

C. Mazengarb, Mineral Resources Tasmania, PO Box 56, Rosny Park, Tasmania 7018, Australia.

A. Nicol, C. Uruski, and L. Wallace, GNS Science, PO Box 30368, Lower Hutt, New Zealand. (a.nicol@gns.cri.nz)

G. Rait, Talisman Energy, 3400, 888 3rd St SW, Calgary, Alberta, Canada T2P 5C5.